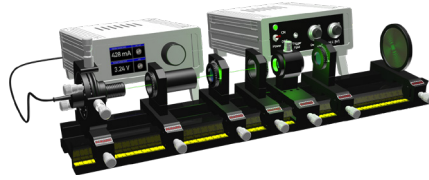


PE - Optical Experiments

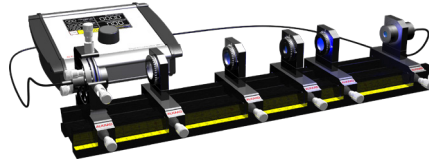
PE-0100 Double Refraction of Light

13



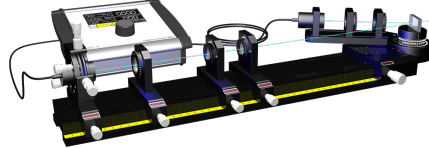
PE-0200 Polarisation of Light

15



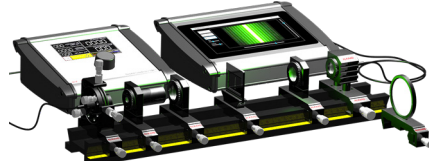
PE-0300 Reflection and Transmission

17



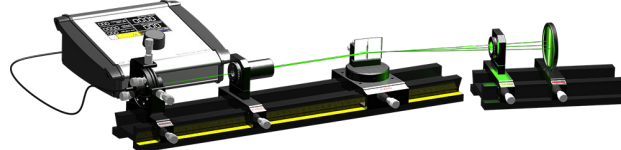
PE-0400 Diffraction of light

19



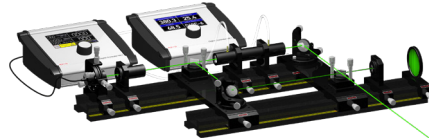
PE-0500 Interference of Light

20



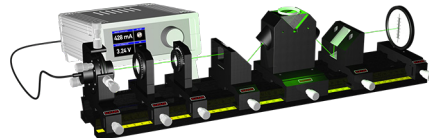
PE-0600 Optical Interferometer

22



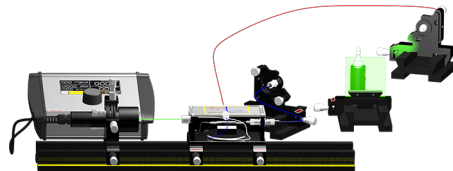
PE-0700 Abbe Refractometer

24



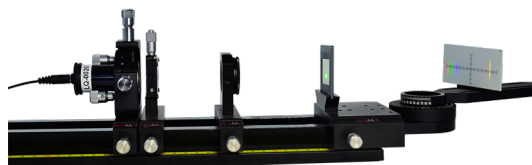
PE-0800 Holography

25



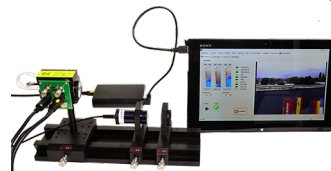
PE-0900 Diffraction Grating

27



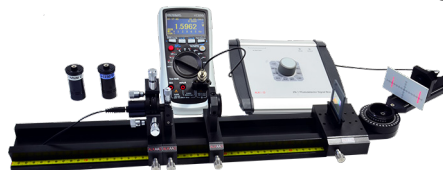
PE-1000 Camera and Imaging

28



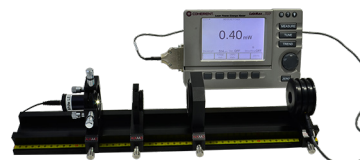
PE-1100 LED and Diodelaser

29



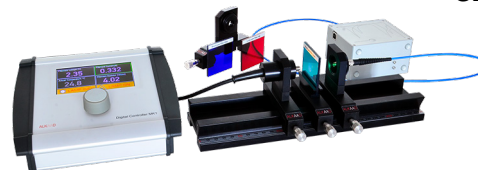
PE-1300 Radio-and Photometry of Light

31



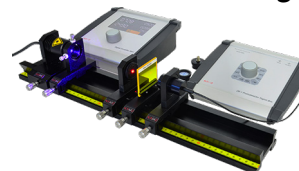
PE-1400 Spectrometer

32



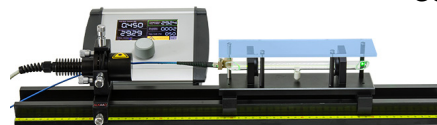
PE-1500 Ruby Excited Lifetime & Spectroscopy

34



PE-1600 Iodine Molecular Spectroscopy

36

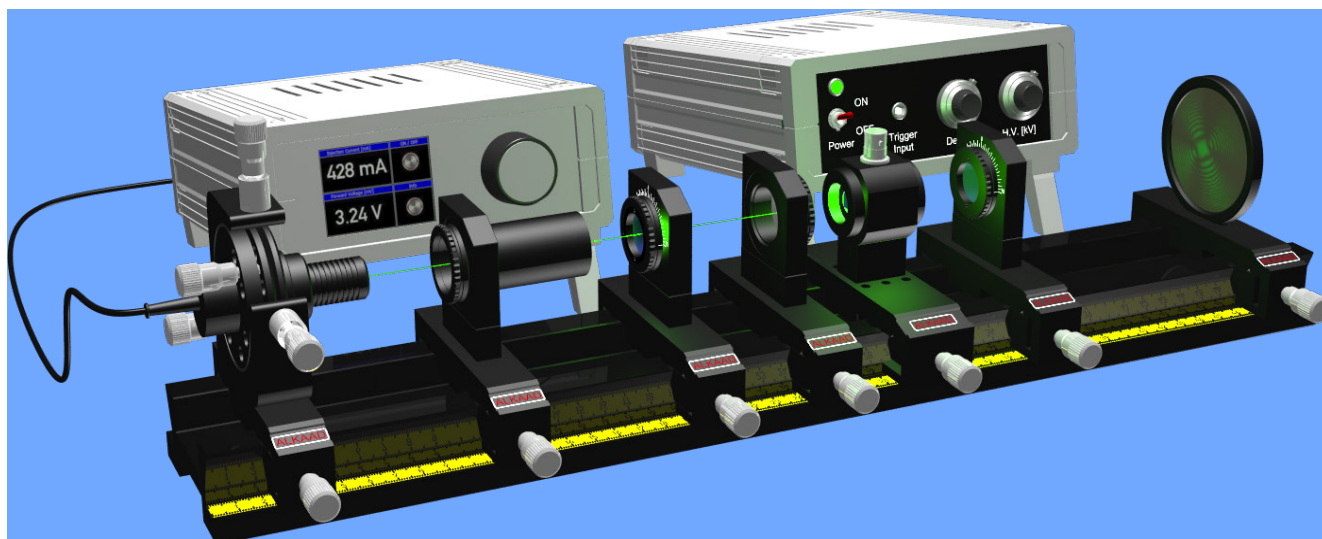


PE-1800 Planck's Law

38



PE-0100 Double Refraction of Light



Birefringence
Conoscopic imaging
Quarter and half waveplate

Ordinary and Extraordinary beam
Crystalline quartz
Pockels Cell

Jones matrix
Iceland Spar (Calcite)



In 1669, Erasmus Bartholin was the first one who reported his observations on double refraction. He investigated a crystal of calcite: not the only crystal which shows double refraction, but a crystal with an extraordinary high markedness of this phenomenon. His discovery and its first scientific explanation by Christian Huygens in 1674 marked the beginning of the studies on optical crystal properties. More than 100 years later, crystal optics

got further insights through Dominique Arago, who studied the polarization and optical activity, and Jean-Baptiste Biot who defined the first principles of crystal optics, by differentiating in particular, uniaxial and biaxial crystals principles which are still valid today. Birefringent materials are important components in optics, for example as half and quarter wave plates, precision polarizer to tune laser lines. The experiments may start with the observation of birefringence shown by calcite crystal. The green

probe laser is directed to the calcite and the splitting of the laser beam in ordinary and extraordinary rays are observed. The polarization of these rays is measured by using the rotary polarisation analyser. As an example of a biaxial crystal a Pockels cell containing a Lithium Niobate crystal is used. In a conoscopic set-up impressive interference pattern are created when the high voltage is applied. Furthermore, the optical retardation for different voltage levels is measured and the half wave voltage is determined.

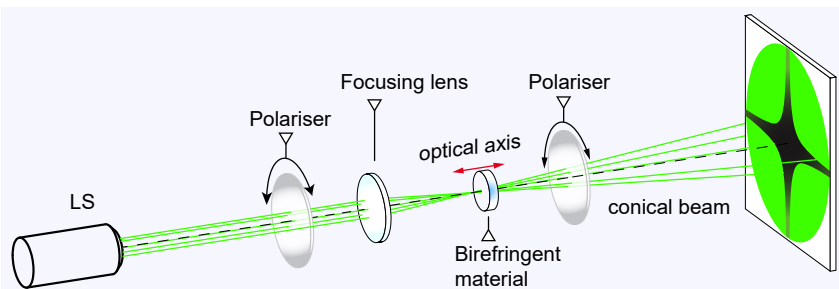


Fig. 1: The optical axis of the birefringent material parallel to the light beam

The creation of a conoscopic image requires a birefringent material where the optical axis is oriented parallel to the incident light beam. In this experiment we are using a laser emit-

ting a wavelength of 532 nm (green). The light passes the first polarizer. A focusing lens creates the "conical" light beam which traverses the birefringent material. The second polarizer

is aligned orthogonally to the first one. In direction of the optical axis, the material behaves isotropic and there will be no change in the polarisation stage of the incident light. The corresponding image on the screen remains dark. All other rays propagating inclined to the optical axis undergo a change to their polarisation in such a way that a fraction can pass the orthogonally oriented polarizer.

Consequently, a typical intensity distribution results which is a fingerprint for the specific birefringent material. Areas with same intensity (same retardation) are termed as isogyres, places of same birefringence. Conoscopy is a very important method to find the optical axis of raw crystals in optic manufacturing as well as quality control for LCD displays.

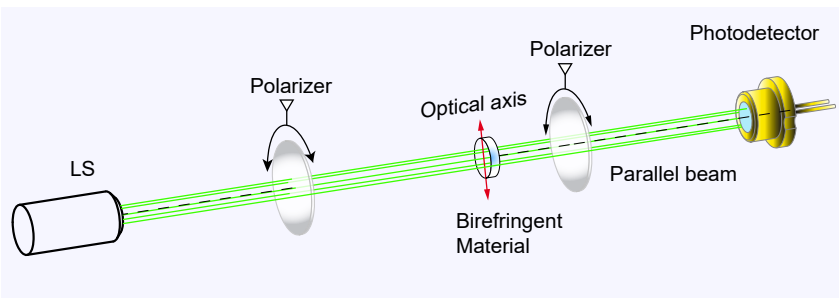


Fig. 4.2: The optical axis of the birefringent material perpendicular to the light beam

Another method to characterise birefringent materials are arrangements where the optical axis of the crystal is perpendicularly oriented to the light source. In such a case, the light is almost parallel. The birefringent material is placed between two rotatable polarizers. By

means of a photodetector, the transmitted intensity is measured as a function of the angle orientation of either the birefringent material or the polarizer. Without any material between the two polarizer the famous Malus' law can be verified.

$$I = I_0 \cdot \cos^2(\vartheta)$$

Whereby ϑ is the angle position between both polarizers. In case they are oriented to the same angle, the value of ϑ is zero and we obtain maximum transmission. In they are orthogonally aligned to each other the value of ϑ is 90° resulting in zero transmission. Placing a half wave plate between the polarizers results in an increase in the transmission. In a certain position the transmission becomes maximum, that means that the half wave plate turns the polarisation by 90° . In the same way we examine the behaviour of a quarter wave plate. It turns out that such a plate converts linear light into circular ones provided the optical axis of the plate is oriented by 45° with respect to the polarisation direction of the light.

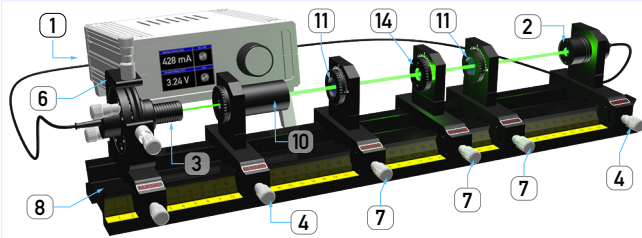
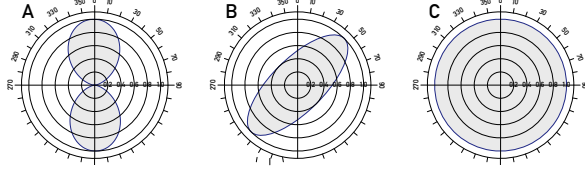


Fig. 4.3: Setup to measure the phase retardation and Malus' law



Double Refraction and Malus' Law

A green laser pointer (3) is used as light source. In a first experiment the polarisation of the probe laser (3) is determined. For this purpose only one polarizer (11) is used. The laser beam is expanded (10) and passes the polarizer (11). By means of the photodetector (2) the intensity of the light behind the second polarizer is detected and the value is displayed on the controller (1). For different angles of the polarizer the intensity is drawn into a graph with polar coordinates. If the laser is linearly polarized we should expect a graph like (A).

To make sure that the laser light is linearly polarized, one polarizer is placed behind the beam expander and turned to maximum intensity. The second polarizer is used as analyser. A angular plot of the intensity will yield the verification of the Malus' law (A). For the next experiment the polarizers are oriented in such a way that the transmitted intensity is almost zero. The quarter waveplate (14) is placed between the polarizer. Depending on the orientation of the waveplate we will get elliptical (B) or circular polarized light (C).

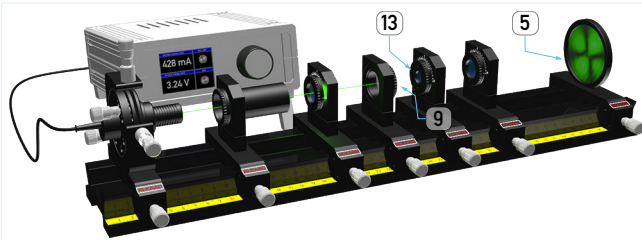


Fig. 4.4: Conoscopic Setup for a quartz crystal plate

Conoscopy with a quartz

By adding the lens (9) in the beam path, the laser beam creates a focus in the distance of its focal length and subsequently it becomes divergent and forms a "cone". A double refractive quartz plate (13) is placed in the so created focal plane. The crystal is cut in such a manner that the optical axis lies perpendicular to the surface of the plate. The divergent beam can be interpreted as a bunch of rays with different propagation angle passing the quartz crystal. All those rays which are retarded by $\lambda/2$ will be blocked by the next polarizer creating a beautiful pattern of dark and bright areas on the screen (5).

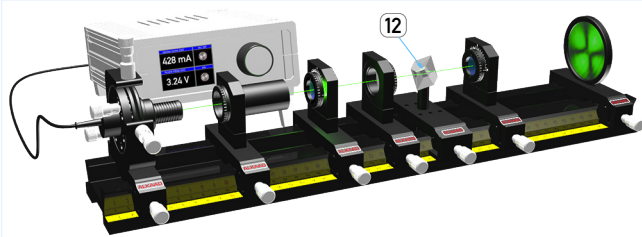


Fig. 4.5: Conoscopic Setup with a calcite crystal

Conoscopy with a calcite crystal

With a value of $\Delta n = 0.172$ calcite crystal has a more than 100 times stronger double refraction than a quartz crystal with has a value of 0.0091.

The optical axis of the calcite crystal goes from the upper left to the lower right corner of the crystal as shown in the picture on the left. Therefore we need to cut the crystal in such a way, that a beam can travel from one corner to the other. Such a crystal is mounted to a post holder to permit the study of the much stronger conoscopic pattern on the screen.

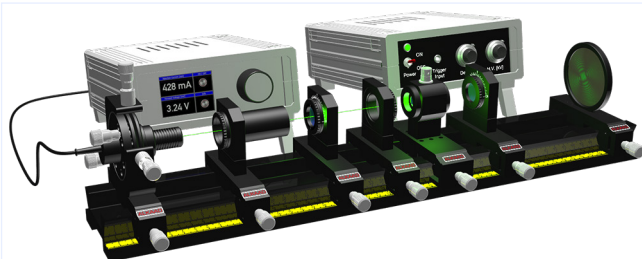
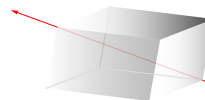


Fig. 4.6: Conoscopic Setup for a Pockels cell

Characterising a Pockels Cell

A Pockels cell is placed in the focal plane of a polarized and a conoscopic beam. By inserting a polarization analyser, beautiful patterns of interference can be observed on a screen and need to be interpreted. When the high voltage to the Pockels cell is switched on, the crystal becomes biaxial and shows other interference patterns, characteristic for such crystals of lower symmetry. Another measurement example is the determination of the half wave voltage. At the lowest applicable voltage the polarisation analyser is turned to maximum intensity. The cell voltage is increased until the transmitted intensity becomes almost zero which is the case when the phase retardation of the cell is $\lambda/2$. In this case, the cell acts as half waveplate.

PE-0100 Double Refraction of Light consisting of:

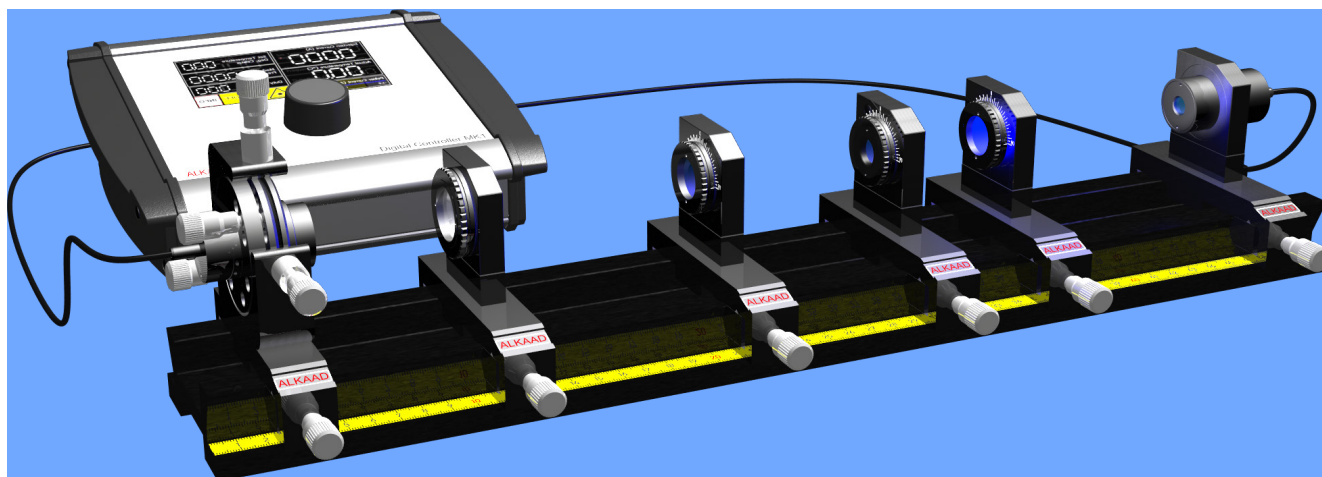
Item	Code	Qty.	Description	Details page
1	DC-0020	1	LED and Photodiode Controller	121 (2)
2	DC-0250	1	Active SiPIN Photodetector	124 (24)
3	LQ-0020	1	Green (532 nm) DPSSL in ø25 housing	119 (1)
4	MM-0020	3	Mounting plate C25 on carrier MG20	93 (1)
5	MM-0024	3	Mounting plate C25-S on carrier MG20	93 (2)
6	MM-0110	1	Translucent screen on carrier MG20	94 (10)
7	MM-0420	1	Four axes kinematic mount on carrier MG20	96 (25)
8	MP-0150	1	Optical Bench MG-65, 500 mm	93 (8)
9	OC-0040	1	Plano-convex lens f=40 mm in C25 mount	99 (4)
10	OC-0360	1	Beam Expander x6 in ø25 housing	100 (17)
11	OC-0710	2	Polarizer in C25 mount	102 (34)
12	OC-0820	1	Calcite crystal on rod and carrier	103 (44)
13	OC-0830	1	Optical quartz plate in C25 mount	103 (45)
14	OC-0840	1	Quarter-wave plate in C25 mount	103 (46)
15	UM-PE01	1	Manual Double Refraction of Light	
Option (order separately)				
16	DC-0358	1	Pockels Cell Driver DQ21	125 (30)
17	OM-0030	1	Lithium Niobate Pockels Celle C-1043	110 (4)

Highlights

Basic experiment
Conoscopy suitable for live demonstration

Intended institutions and users:
Physics Laboratory
Engineering department
Electronic department
Biophotonics department
Physics education in Medicine

PE-0200 Polarisation of Light



Keywords

Optical Activity
Linear Polarized Light
Green Laser
Photodetector

Double Refraction
Elliptical, Circular Polarized Light
Quartz Retarder Plate
Light Power Control

Polarization of Light Sources
LED Light Source
Mica Retarder Plate
Malus' Law

Introduction



In the year 1809, Etienne Malus discovered the polarization of light by reflection and stated a law which describes the intensity distribution of polarized light as a function of the relative orientation of a polarization analyser. At that time his findings were in contradiction to the presumption of light waves being longitudinal rather than transversal. His discovery had far reaching conse-

quences for the wave theory of light, and his unambiguous experimental results launched a big debate, among the leading scientists about the wave properties of light. Finally, as a compromise light was conceded to have transversal as well as longitudinal character. Two years later Dominique Arago investigated a sample of quartz and discovered its optical activity, a property of many natural and also synthetic materials. Later on, Augustine Fresnel could

explain the effect of optical active materials on light by introducing the phenomenon of circular birefringence. In this series of experiments the polarization state of the light sources in use is determined. Furthermore, polarized light is used to prove the Malus' and Fresnel's Laws with respect to their states on polarization. The influence of crystal wave plates and optically active materials on polarization is studied.

How it works

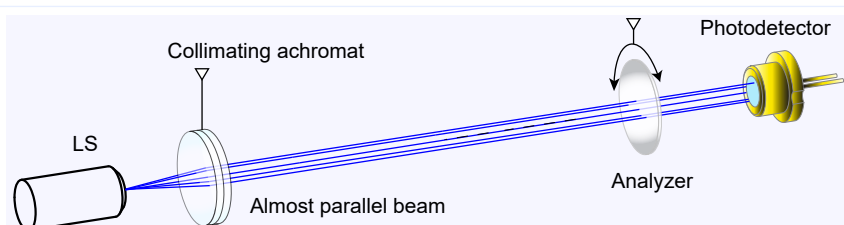


Fig. 4.7: Basic setup to measure the polarisation of a light source LS

As light source either as coherent "green" laser or a blue or white light emitting LED is used. In case of using a LED an achromat is used to form an almost parallel beam. By means of a polarisation analyser and the photodetector the intensity of the light source as function of the analyser angle is measured. As a result, three plots are created representing the polarisation of the green laser and the blue and white LED.

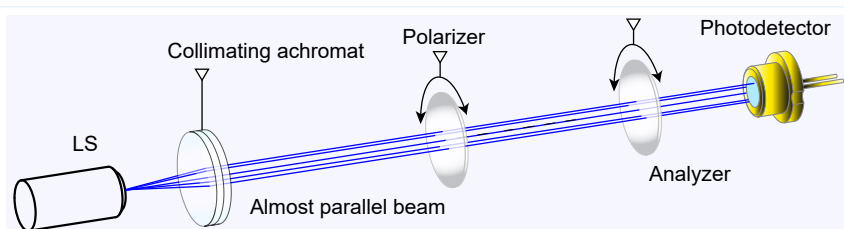


Fig. 4.8: Setup to measure the Malus's law

By using an additional polarizer the emitted light is polarised. If the analyser angle is set to 90 degrees with respect to the polarizer the passed intensity is a minimum and for 0 degree a maximum. Between these values the transmitted intensity behind the analyser is according to the Malus' law. This setup allows the verification of Malus's law and demonstrates furthermore an arrangement to change the intensity of a light source without changing the operating current.

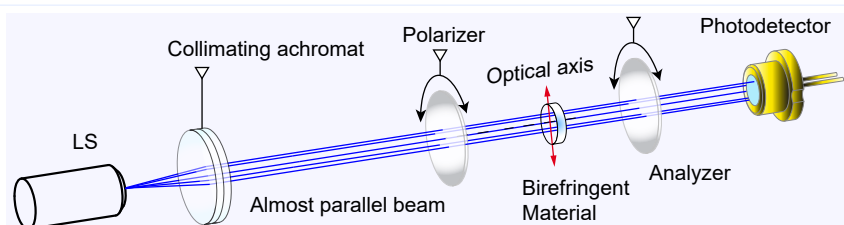


Fig. 4.9: Placing birefringent material between two crossed polarizer

Materials which change the polarisation of transmitted light are termed as optical active. Such natural materials are for instance crystalline quartz, calcite or mica. Within the frame of this experiment three crystalline plates made of quartz and mica are used. The plates are mounted in a click mount with an index mark. The plate is placed behind the polarizer and the transmitted intensity is measured as function of the analyser angle. The resulting angular intensity plot informs about the particular optical activity.

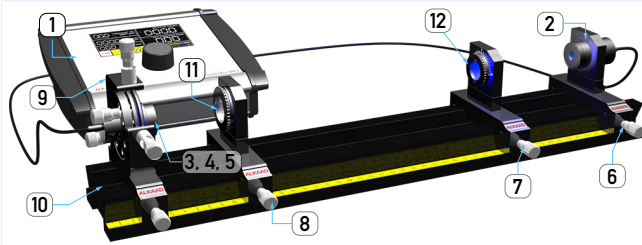


Fig. 4.10: Setup to measure the polarisation of the light source

Measurement of the Light Source

As light source either the blue (5) or white (4) or the “green” laser (3) is used. The light source is clicked into the four axes kinematic mount (9) and connected to the LED and photodiode controller (1). Each light source has an embedded non-volatile memory into which the property of the light source is stored. The information is processed and displayed by the controller (1) to ensure the operation of the attached light source within its allowed parameter. In addition, the controller contains a pre-amplifier and processing stage for the attached photodiode. The settings are selected by means of the touch screen and set by the precision digital settings knob. The measurements starts with the characterization of the light source as intensity versus injection current and versus the analyser (12) angle.

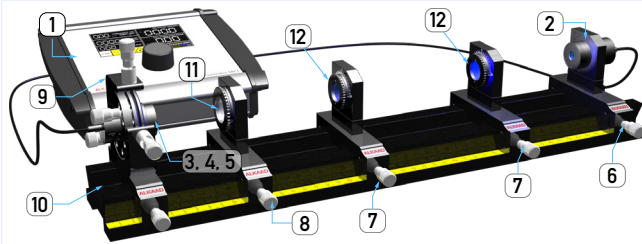


Fig. 4.11: Malus' Law and optical power control

Malus' Law and Optical Power Control

The achromat (11) is used to collimate the radiation of the LED to obtain an almost parallel light beam. To make sure that the light is linearly polarized, the first polarizer (12) is placed behind the collimator (11) and turned to maximum intensity. The second polarizer (12) is used as analyser. The transmitted intensity is measured by means of the photodetector (2) and the controller (1). A angular plot of the intensity yields the verification of the Malus' law. Such an arrangement is often used to control the intensity of a light source when the change of the emission wavelength by the control of the injection current is not desired.

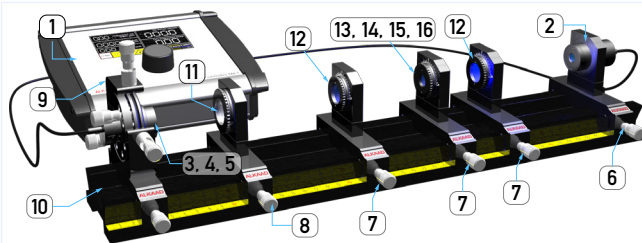


Fig. 4.12: Demonstration and measurement of optical activity

Polarisation by Optical Activity

To demonstrate the effect of double refraction or birefringence on the polarisation of the transmitted light beam 4 different optical active materials are used.

- (14) Plate of crystalline quartz
- (15) Quarter-wave plate made from quartz
- (16) Half-wave plate made from quartz
- (13) Plate of natural mica

The plates are mounted into a click 25 mount with an index mark and the mounting plate (7) provides the corresponding angle scale. The first polarizer is set to maximum intensity. The resulting linear polarised light of the light source (3, 4, 5) passes the inserted plate and undergoes a phase retardation depending on the kind and orientation of the birefringent material.

The measured results can be plotted either in Cartesian or polar coordinates. Below the Fig. 4.12 such an example in polar coordinates is shown for:

- A. Linear polarized
- B. Elliptical polarized
- C. Circular polarized light

PE-0200 Polarisation of light consisting of:

Item	Code	Qty.	Description	Details page
1	DC-0020	1	LED and Photodiode Controller	121 (2)
2	DC-0120	1	Si-PIN Photodetector, BPX61 with connection leads	123 (15)
3	LQ-0020	1	Green (532 nm) DPSSL in ø25 housing	119 (1)
4	LQ-0200	1	White LED in ø 25 Housing	119 (6)
5	LQ-0230	1	Blue LED in ø 25 housing	120 (12)
6	MM-0020	1	Mounting plate C25 on carrier MG20	93 (1)
7	MM-0024	3	Mounting plate C25-S on carrier MG20	93 (2)
8	MM-0030	1	Mounting plate C30 on carrier MG20	93 (4)
9	MM-0420	1	Four axes kinematic mount on carrier MG20	96 (25)
10	MP-0150	1	Optical Bench MG-65, 500 mm	93 (8)
11	OC-0140	1	Achromat f=40 mm in C30 mount	99 (9)
12	OC-0710	2	Polarizer in C25 mount	102 (34)
13	OC-0810	1	Mica plate in C25 mount	103 (43)
14	OC-0830	1	Optical quartz plate in C25 mount	103 (45)
15	OC-0840	1	Quarter-wave plate in C25 mount	103 (46)
16	OC-0850	1	Half-wave plate in C25 mount	103 (47)
17	UM-PE02	1	Manual Polarisation of Light	

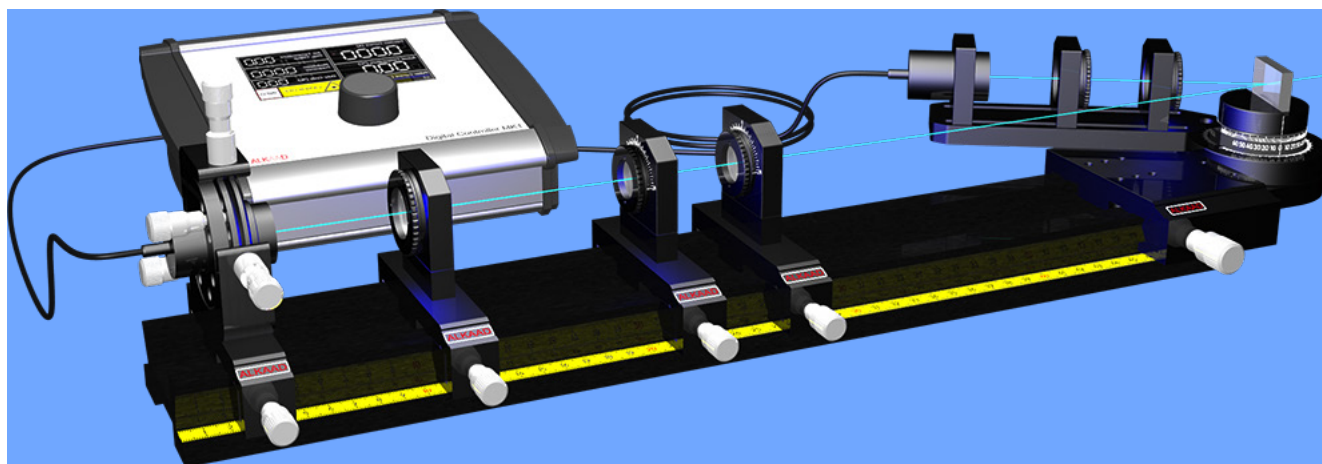
Highlights

Basic experiment

Intended institutions and users:

- Physics Laboratory
- Engineering department
- Electronic department
- Biophotonics department
- Physics education in Medicine

PE-0300 Reflection and Transmission



Reflection Law
Transmittance
Brewster Angle

Fresnel Laws
Polarization
LED Characterization

Reflectance
Anti-Reflection Coating
Green Laser Properties



Reflection of light on surfaces is a familiar phenomenon of daily life. Therefore it is no surprise that the reflection law is one of the well known optical laws and was first stated by Ibn Al Haitham in the beginning of the 10th century. Little was commonly known about polarization of light and its connection with reflection and refraction. This connection is formulated in the Fresnel Laws which

are usually expressed as transmittance and reflectance as a function of the index of refraction and angle of reflection. The four formulas which were deduced by Augustin Fresnel in 1821 contain the complete theory of reflection, refraction and polarization of isotropic materials. The fundamental understanding of reflection and transmission is essential for the design of laser mirrors, sun glasses and a lot more. By dielectric coating, such components are made

either to optimise or to suppress reflection. Within this experiment the reflection law is verified using a metal coated mirror. The next part covers the quantitative verification of the Fresnel Laws on a specially shaped glass plate using polarized light. Finally the spectral performance of a dielectric coated mirror is investigated using a white LED and a grating.

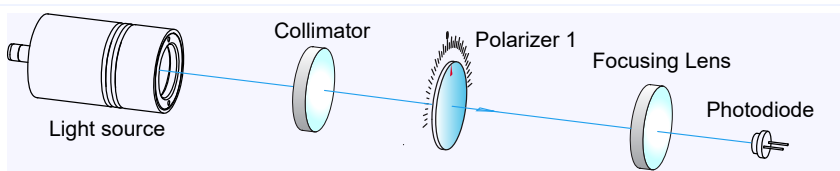


Fig. 4.13: Characterising the light source

As source a white light LED and a “green” laser are used. Both sources are characterised by measuring the optical power versus the injection current. In case of the LED, a collimator is used to obtain an almost parallel light beam. Furthermore, the spatial intensity distribution of the LED can be measured when using the provided goniometer.

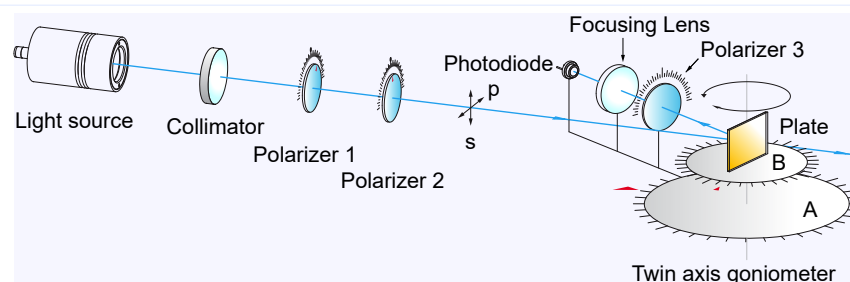


Fig. 4.14: Arrangement to measure reflected and transmitted light

The light of either a white light LED or “green” laser is strongly polarised by means of polarizer 1 and 2 and hits the probe plate. When using the LED, a collimator lens creates an almost parallel light beam. The optical plate is attached to the goniometer plate B and can be rotated by 360°. The photodiode along with a focussing lens and the polarizer 3 are attached to the arm of goniometer A. By turning of B a defined angle of incidence is set. The arm of goniometer A is turned in such a way that the signal detected by the photodiode becomes maximum. In this way the Snell’s or reflection law is verified. To verify the Fresnel’s equations, the polarisation state of the incident light is set to either “s” (perpendicular) or “p” (parallel) with respect to the plane of incidence which is spanned by the vector of the incoming and reflected beam.

parallel light beam. The optical plate is attached to the goniometer plate B and can be rotated by 360°. The photodiode along with a focussing lens and the polarizer 3 are attached to the arm of goniometer A. By turning of B a defined angle of incidence is set. The arm of goniometer A is turned in such a way that the signal detected by the photodiode becomes maximum. In this way the Snell’s or reflection law is verified. To verify the Fresnel’s equations, the polarisation state of the incident light is set to either “s” (perpendicular) or “p” (parallel) with respect to the plane of incidence which is spanned by the vector of the incoming and reflected beam.

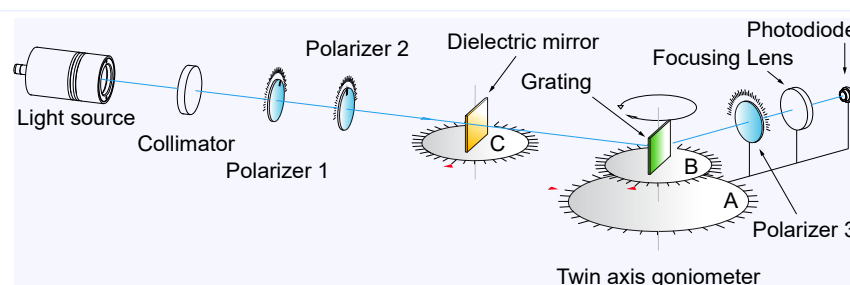


Fig. 4.15: Setup for measuring the spectral transmittance of a mirror

Optical components, especially mirrors are extremely important in photonics. Meanwhile a variety of technologies exist to tailor the spectral behaviour of optical surfaces like short

pass, long pass or even ultra narrow band pass mirrors. The aim of this experiment is the spectral characterization of such a mirror. As light source a white light LED and for the spectral

resolution, a transmission grating is used. The dielectric mirror is attached to a turntable (C) to measure the spectral response also for different angle of incidence. The grating is attached to the goniometer B, where it is kept at an angle of zero degrees with respect to the direction of the probe light beam. The arm of goniometer A is turned to the first or second order of the grating. The first measurement is carried out without the dielectric mirror to record the spectrum of the white light emitting LED. The second measurement is performed including the dielectric mirror. The spectral transmittance of the dielectric mirror is obtained by normalising the values of the second measurement to the first measurement.

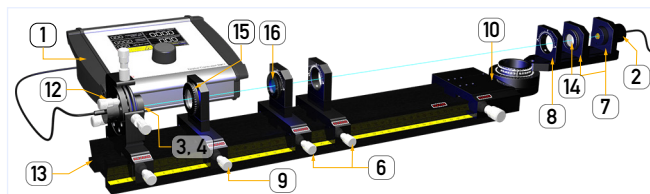


Fig. 4.16: Characterising the light source

The aim of this setup is the measurement of the optical power of the provided white light LED and the “green” laser versus the injection or operation current. By means of the LED and laser controller (1) the individual current can be set from zero to the maximal permissible value. The output power is measured by the photodiode (2) which is connected also to the controller (2). The built-in amplifier and microprocessor converts and displays the measured photo current. In a next measurement the polarisation of the LED and the green laser is measured by rotating the polarizer (16) in its holder whereby the optical power is measured.

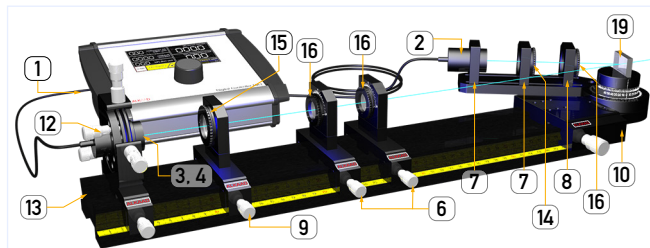
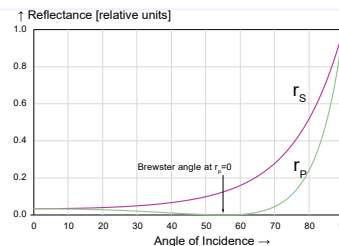


Fig. 4.17: Setup to verify the Snell's (reflection) and Fresnel's Law

With this setup the angle and polarisation dependent reflection or transmission of a probe (19) is measured. The probe, which can be either a glass plate or a front face mirror is placed into the fixed arbor receptacle of the twin axis goniometer (10). The probe body has an index mark for reading its angle with respect to the scale of the arbor receptacle. The second goniometer provides an arm onto which the photodetector (2), a focussing



lens (14) and a polarizer (16) are mounted. As light source either the green laser or the white LED is used. When using the LED the additional collimator (15) is used to obtain an almost parallel LED light beam. With the pair of polarizers the desired polarisation *s* or *p* are adjusted.

For different incident angles the reflected intensity is measured by the photodiode (2) and the control unit (1). The plot of the data as intensity against the angle of incidence verifies the Fresnel equations. For an index of refraction of 1.45 these values are calculated and shown in the figure above. The angle of incidence for which the reflected intensity I_p becomes zero is termed as Brewster angle which is highly important for all those applications where the losses due to reflection should be zero.

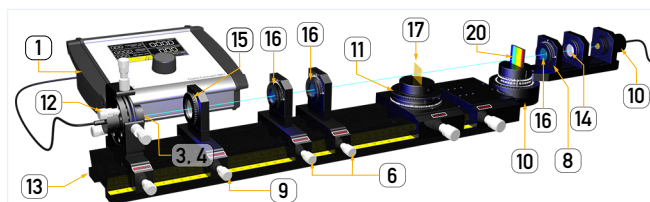
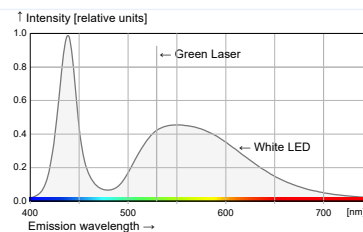
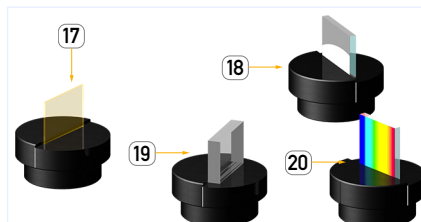


Fig. 4.18: Measuring the spectral transmittance

By placing a transmission grating (20) into the fixed arbor receptacle of the goniometer (10) the setup is converted into a simple spectrometer. To measure the spectral property of the dichroic mirror (17) it makes sense to use the white light emitting LED. The emission wavelength of the LED ranges from 400 - 700 nm. The mirror (17) is inserted into the



centre hole of the carrier with rotation stage (11). By turning the goniometer arm the photodetector measures the intensity as a function of the angle. The measurements can be performed in the first or second order of the transmission grating. A first measurement is performed without the mirror (17) to obtain the spectral curve of the LED. In a subsequent measurement with inserted mirror (17) the influence of the mirror becomes apparent. The spectral curve of the mirror (17) is obtained by dividing the data of the second measurement with the data of the first measurement.



The experiment comes with four different optical modules (OM). A dichroic mirror (17) reflects in the blue range and transmits in the red spectral range. The dichroism depends on the angle of incidence, which will be measured in the experiment. The front face mirror (18) has a metallic coating and is used as general purpose reflector. The mirror is used for the verification of Snell's law. For the measurement

and verification of the Fresnel equations and Brewster's angle, an optical polished glass plate (19) is used. A transmission grating (20) with 600 lines per millimetre is used for the spectral analysis. All components are mounted to a solid base which fits either into the goniometer (10) or into the carrier with rotary stage (11). The index mark serves to measure the angle of incidence when inserted into the respective holder.

PE-0300 Reflection and Transmission consisting of:

Item	Code	Qty.	Description	Details page
1	DC-0020	1	LED and Photodiode Controller	121 (2)
2	DC-0120	1	Si-PIN Photodetector, BPX61 with connection leads	123 (15)
3	LQ-0020	1	Green (532 nm) DPSSL in ø25 housing	120 (10)
4	LQ-0200	1	White LED in ø 25 Housing	119 (6)
5	MM-0020	1	Mounting plate C25 on carrier MG20	93 (1)
6	MM-0024	2	Mounting plate C25-S on carrier MG20	93 (2)
7	MM-0026	2	Mounting plate 40, C25	
8	MM-0028	1	Mounting plate C25-S with angle gradation	93 (3)
9	MM-0030	1	Mounting plate C30 on carrier MG20	93 (4)
10	MM-0300	1	Carrier with 360° rotary arm	95 (20)
11	MM-0380	1	MG65 carrier with rotary stage	96 (23)
12	MM-0420	1	Four axes kinematic mount on carrier MG20	96 (25)
13	MP-0150	1	Optical Bench MG-65, 500 mm	93 (8)
14	OC-0060	1	Biconvex lens f=60 mm in C25 mount	99 (5)
15	OC-0140	1	Achromat f=40 mm in C30 mount	99 (9)
16	OC-0710	3	Polarizer in C25 mount	102 (34)
17	OM-0310	1	Dichroic mirror on rotary table	111 (11)
18	OM-0320	1	Front face mirror on rotary table	112 (12)
19	OM-0330	1	Glass plate on rotary table	112 (13)
20	OM-0340	1	Transmission grating on rotary table	112 (14)
21	UM-PE03	1	Manual Reflection & Transmission	

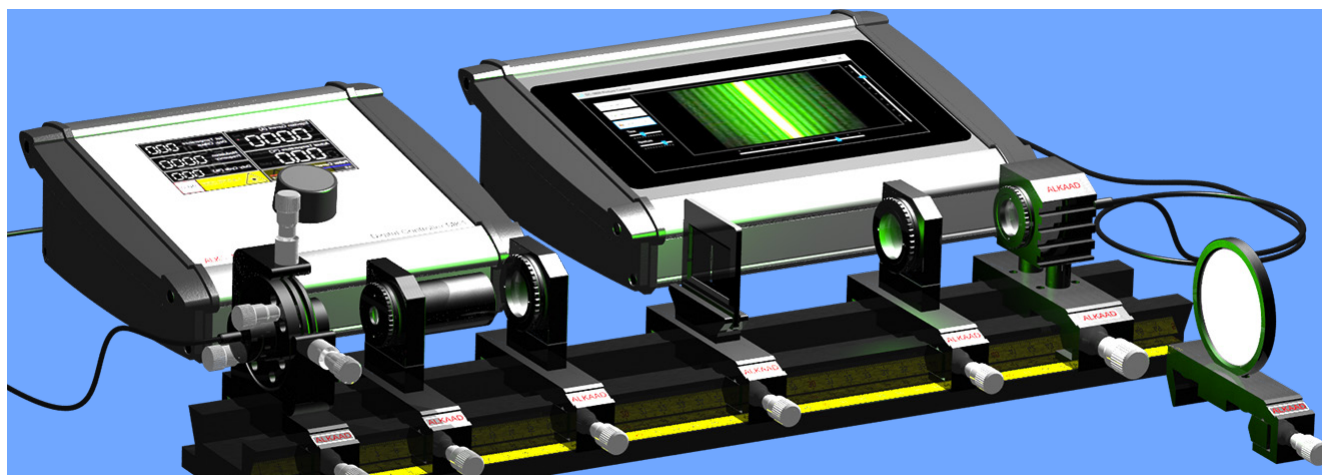
Highlights

Basic experiment

Intended institutions and users:

Physics Laboratory
Engineering department
Electronic department
Biophotonics department
Physics education in Medicine

PE-0400 Diffraction of light



Huygens Principle Diffraction at a Wire



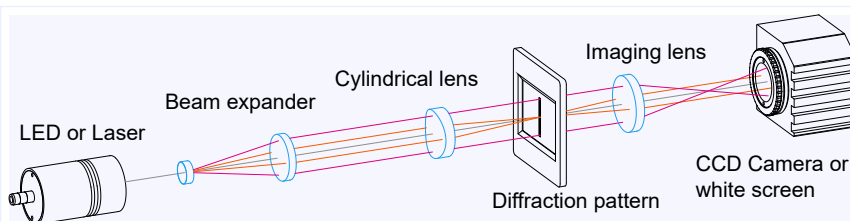
All objects which restrict the free propagation of light cause diffraction. Although this phenomenon is always present, it is usually neglected, because the effect is too insignificant for the topic of investigation. But if light hits sharp edges, diffraction will appear clearly and cannot be neglected, especially when light is diffracted on very narrow openings like

Single and Multiple Slits Babinet Theorem

holes or slits. Christian Huygens formulated his observation of diffraction in the 17th century applying the principle of elementary waves. In 1800 Fresnel and Fraunhofer both studied the effect of diffraction in detail. Fresnel used divergent light for his investigations, whereas Fraunhofer used parallel light created by a pair of lenses. Both techniques are termed as Fresnel and Fraunhofer diffraction respectively. This experiment of

Diffraction of LED Light Diffraction of Coherent Light

fers both types of diffraction. Experiments are performed using monochromatic laser light which will be diffracted at slits and holes of various widths. Thin wires impressively prove the Babinet theorem which states that complementary masks (slit, wire) result in the same diffraction pattern. The obtained diffraction patterns are imaged on a white screen and the pattern can also be recorded by a CCD camera.



The figure on the left shows the arrangement using a laser. In case a LED is used, the Beam expander is exchanged against a collimating lens. To obtain crisp diffraction fringes most of the light should hit the diffraction pattern. In case of using a slit, an extra cylindrical lens is used to convert the round beam into a line structure. When demonstrating the diffraction at a hole the round laser beam is used as it is.

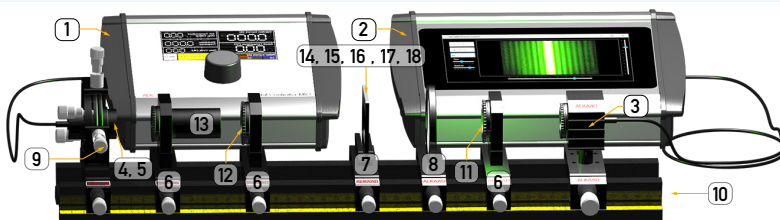


Fig. 4.19: Description of the components

PE-0400 Diffraction of Light consisting of:

Item	Code	Qty.	Description	Details page
1	DC-0020	1	LED and Photodiode Controller	121 (2)
2	DC-0800	1	CCD Camera Controller	126 (33)
3	DC-0820	1	CCD Camera Module	126 (34)
4	LQ-0020	1	Green (532 nm) DPSSL in ø25 housing	119 (1)
5	LQ-0210	1	Red LED in ø 25 housing	119 (7)
6	MM-0020	3	Mounting plate C25 on carrier MG20	93 (1)
7	MM-0060	1	Filter plate holder on MG20	94 (7)
8	MM-0110	1	Translucent screen on carrier MG20	94 (10)
9	MM-0420	1	Four axes kinematic mount on carrier MG20	96 (25)
10	MP-0150	1	Optical Bench MG-65, 500 mm	93 (8)
11	OC-0040	2	Plano-convex lens f=40 mm in C25 mount	99 (4)
12	OC-0280	1	Cylindrical lens f=80 mm in C25 mount	100 (15)
13	OC-0360	1	Beam Expander x6 in ø25 housing	100 (17)
14	OC-0470	1	Wire 0.05 mm in 50x50 mm frame	101 (23)
15	OC-0480	1	Circular apertures in 50x50 mm frame	101 (24)
16	OC-0482	1	Gauze 300 mesh in 50x50 mm frame	101 (25)
17	OC-0484	1	Single slit 0.06 mm in 50x50 mm frame	101 (26)
18	OC-0486	1	Double slit in 50x50 mm frame	101 (27)
19	UM-PE04	1	Manual Diffraction of Light	

Within the experiment a red emitting LED (5) or a green emitting laser (4) are used. For both light sources the controller (1) provides the individual current and voltage. The controller's microprocessor reads the property of the connected light source and sets the parameter accordingly. When using the green laser and a vertical slit (17,18) or wire (14), the beam expander (13) is needed to create in conjunction with the cylindrical lens (12) a vertical line shape. Different types of diffraction elements can be inserted to the plate holder (7). To verify the Babinet's theorem a slit (17) and a wire (14) with same dimensions is used. Furthermore the diffraction fringes a double slit (18), a circular aperture (15) and a two dimensional structure (16) are created and recorded. For a first view, the translucent screen (8) is used. The fringes on the screen are recorded by the high resolution (8 MP) CCD camera (3) and are displayed live on the digital video controller (2). The image can be taken as still photo or as video. The video controller provides USB inputs for a memory stick or other external devices like mouse or keyboard. The HDMI output allows the connection to a projector in the lecture hall to demonstrate a live experiment.

Highlights

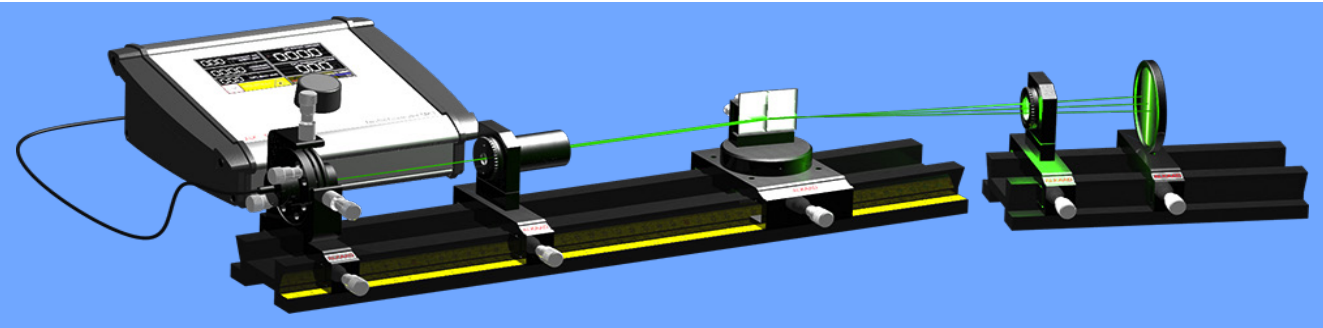
Basic experiment

Suitable for live demonstration!


Intended institutions and users:

Physics Laboratory
Engineering department
Electronic department
Biophotonics department
Physics education in Medicine

PE-0500 Interference of Light



Fresnel's Mirror Optical Resonator Fresnel's Zone Plate	Newton's Rings Spatial / Temporal Coherence Diffraction	Fabry Perot Plate Coherence Length Interference
--	--	--



Interference of light, although very common in almost all fields of optics, is not always easily observed, often overlooked or just neglected. When Isaac Newton did his investigations on optics, he described interference observations in detail. But only Thomas Young was on the right way of interpretation when he stated the general law of constructive and destructive interference of light in

1801 and when he gave the experimental proof of interference of light in 1802. His work had influential consequences in considering light as a wave. On one hand interference is an impressive way to demonstrate the wave character of light, on the other hand, many optical instruments are based on interference, e.g. instruments for exact determination of distances or the wavelength of light, so called interferometers. This experiment provides the famous

Fresnel mirror dividing one light beam source into two and superimpose their coherent portions. As a must the Newton's rings module demonstrates interference caused by thin layers. Further on a Fresnel plate is used to illustrate imaging based on interference and finally, a Fabry Perot plate demonstrates the working principle of an optical cavity.

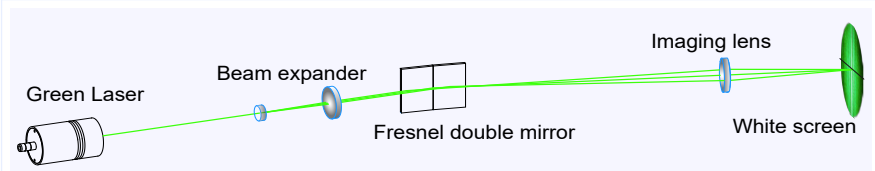


Fig. 4.20: Fresnel's double mirror setup

The laser beam of the green laser is expanded and hits the first mirror in grazing incidence in such a way that one half of the beam is deflected by the first and the other half by the second mirror. The second mirror is slightly tilted against the first one. Both beams are imaged via an expanding lens onto a white screen. In the overlap area of both beams the famous Fresnel interference becomes visible.

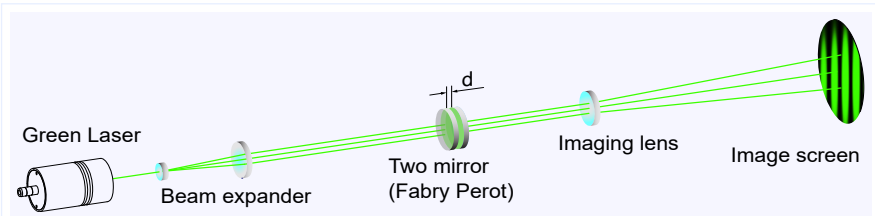


Fig. 4.21: Interference with a Fabry Perot setup

Two flat mirrors are aligned parallel to each other by a spacer forming a Fabry Perot cavity with a mirror distance d of 3 mm with a free spectral range of 50 GHz. The green laser is connected to the control unit to allow the precise tuning of the temperature. Since the frequency change of the green laser is 4.5 GHz per °C we will observe the frequency change as shift of the interference fringes on the screen.

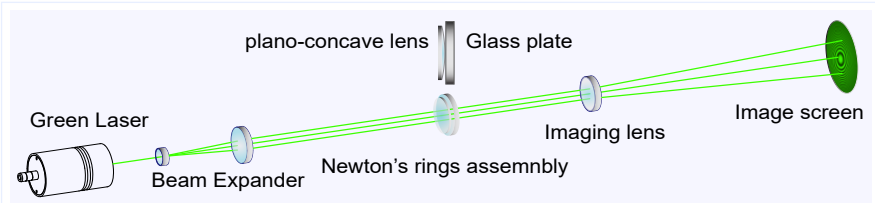


Fig. 4.22: Demonstration of Newton's rings

The classical experiment "Newton's rings" comes with a combination of a glass plate and a plano-concave lens. It is illuminated with a green laser whose beam diameter is enlarged by a beam expander. The interference pattern is imaged onto a white screen. The figure shown on the left shows the setup for observing the fringes in transmission. For observing in reflection direction, an image screen with a small centre hole is used, which is located behind the beam expander.

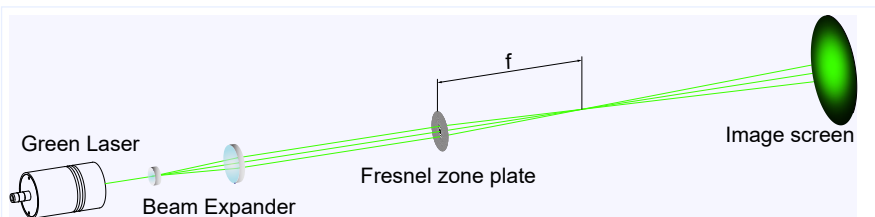


Fig. 4.23: Focusing a laser beam with a Fresnel zone plate

It is amazing to learn that an arrangement of concentric rings shows almost the same property as a lens. For such an arrangement, a Fresnel zone plate is designed in such a way that it will create a lens like image with a focal length of 60 mm. The plate is illuminated with a green laser whose beam is enlarged by a beam expander.

Keywords

Introduction

How it works

Optics Experiments

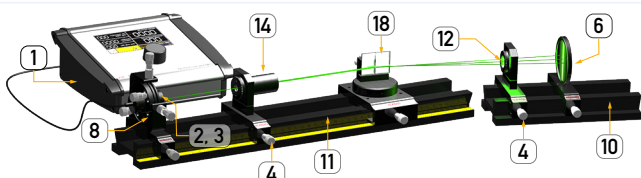


Fig. 4.24: Demonstrating the Fresnel's double mirror interference

As light source a green laser (2) is used, which is mounted into a four axes adjustment holder (8). The beam diameter is enlarged by the 6 x beam expander (14) which is inserted into a mounting plate (4) attached to a carrier. Both mirrors of the Fresnel mirror assembly (18) are independently adjustable from each other. One half of the laser beam hits the first mirror in grazing incidence and the other half the second mirror and both are directed out of the optical axis of the rail. The biconcave lens (12) which is inserted into a mounting plate (4) on an extra rail (10) expands both beams and images them onto the translucent screen (6).

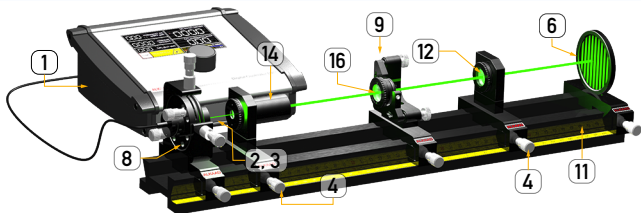


Fig. 4.25: Setup of the Fabry Perot

A pair of two reflective coated glass plates are mounted with a fixed distance of 3 mm into a click 25 holder (16) and mounted into an adjustable

mount (9) to align the Fabry Perot (16). The expanded laser beam (14) of the green laser (2) is directed to Fabry Perot (16). The transmitted beam is expanded by a biconcave lens (12) and imaged onto the translucent screen (6) where the interference pattern becomes visible. Since the wave fronts behind the beam expander are plane (parallel beam) the fringes appear as lines and their distance to each other is given by the wavelength of the light source, the distance of the plates and finally the geometry like expansion of the setup. To study the effect of the wavelength, the temperature of the green laser is changed ($0.004 \text{ nm/}^\circ\text{C}$) by the controller (1) which results in an observable movement of the fringes.

To observe circular fringes, the beam expander can be adjusted for divergent beams.

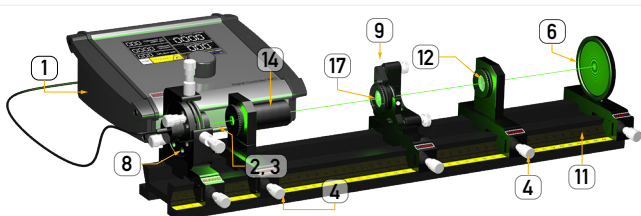


Fig. 4.26: Observation of Newton's rings in transmission

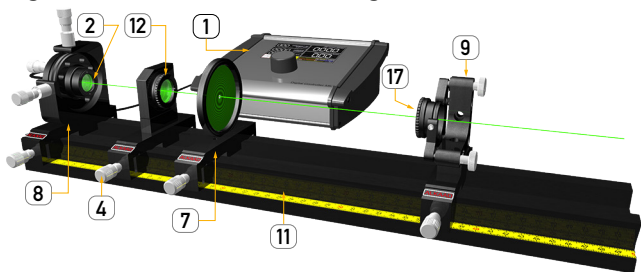


Fig. 4.27: Setup to observe Newton's rings in reflexion

The Newton's ring assembly (17) consists of a plano-convex lens the curved side of which touches a glass plate whereby the flat surface of the lens is parallel to the surface of the glass plate and is used instead of the Fabry Perot (16) of the previous setup. The setup can be operated by using either the green laser (2) or the white light LED (3). In the latter case the collimating achromat (5 and 13) is used instead of the beam expander (14). The beam is expanded by the biconcave lens (12) and imaged onto the translucent screen (6). The observable interference is a result of the superimposition of reflected and transmitted beams of uncoated surfaces, thus the contrast in transmission is comparably low.

A better way to view the Newton's ring with enhanced contrast is to observe the fringes in reflection. In principle a glass plate under an angle of 45° is placed in front of the Newton's ring optics (17). The returning light and therewith the interference pattern is deviated as well and can be displayed on a screen. However, in this setup we are using a white screen (7) with a small central hole which is large enough to pass the incident light. By aligning the Newton's ring optics (17) with the adjustment holder (9) the reflected interference pattern is centred to the screen. To enlarge the image on the screen (7) the imaging lens (12) is used which makes the incident laser beam divergent.

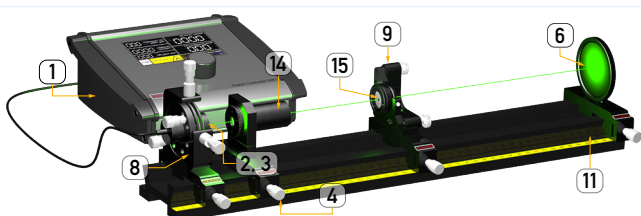
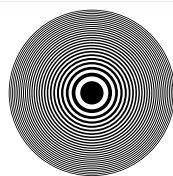


Fig. 4.28: Experiment with Fresnel's zone plate



A zone plate is an arrangement of concentric rings resulting in a focusing ability whose mode of operation is based on diffraction and interference. The thickness and separation of the rings determines its focal length. The image of such a zone plate can be calculated and exposed to high resolution films as used in printing processes. Such a film carrying a zone structure resulting in a focal length of 60 mm is mounted into a click 25 holder (15) and placed into the adjustment holder (9). With the screen (6) the focus of the initial parallel green laser beam is measured.

PE-0500 Interference of light consisting of:

Item	Code	Qty.	Description	Details page
1	DC-0020	1	LED and Photodiode Controller	121 (2)
2	LQ-0020	1	Green (532 nm) DPSSL in $\varnothing 25$ housing	119 (1)
3	LQ-0200	1	White LED in $\varnothing 25$ Housing	119 (6)
4	MM-0020	2	Mounting plate C25 on carrier MG20	93 (1)
5	MM-0030	1	Mounting plate C30 on carrier MG20	93 (4)
6	MM-0110	1	Translucent screen on carrier MG20	94 (10)
7	MM-0114	1	White screen with centre hole	94 (11)
8	MM-0420	1	Four axes kinematic mount on carrier MG20	96 (25)
9	MM-0440	1	Kinematic mount $\varnothing 25.4$ mm on MG20	96 (26)
10	MP-0130	1	Optical Bench MG-65, 300 mm	93 (7)
11	MP-0150	1	Optical Bench MG-65, 500 mm	93 (8)
12	OC-0020	1	Biconcave lens $f=-20$ mm in C25 mount	98 (3)
13	OC-0140	1	Achromat $f=40$ mm in C30 mount	99 (9)
14	OC-0360	1	Beam Expander x6 in $\varnothing 25$ housing	100 (17)
15	OC-0720	1	Fresnel zone plate in C25 mount	102 (35)
16	OC-0730	1	Fabry Perot plate in C25 mount	102 (36)
17	OC-0740	1	Newton's rings optics in C25 mount	102 (37)
18	OM-0450	1	Fresnel mirror assembly	112 (17)
19	UM-PE05	1	Manual Interference of Light	

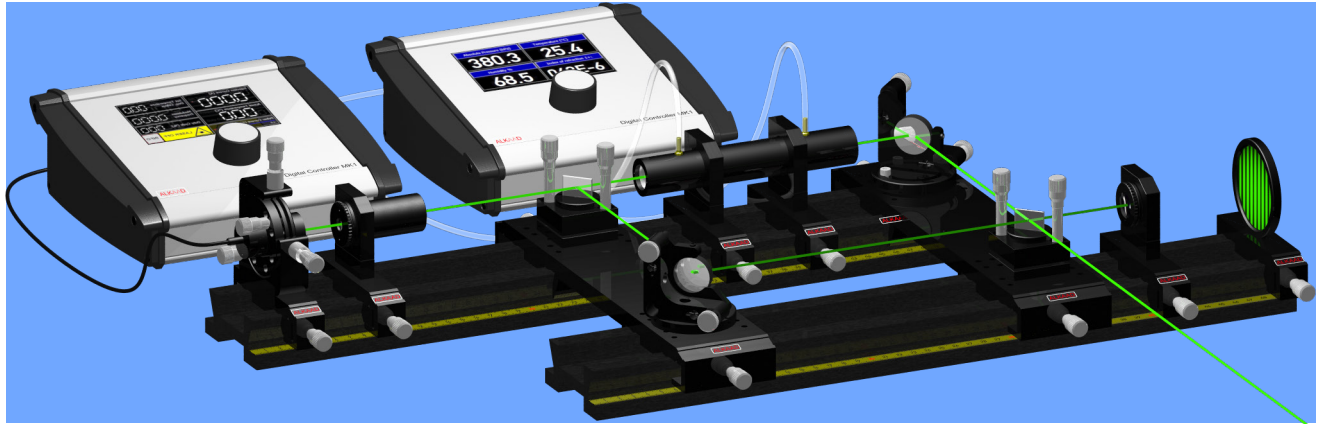
Highlights

Basic experiment

Intended institutions and users:

Physics Laboratory
Engineering department
Electronic department
Biophotonics department
Physics education in Medicine

PE-0600 Optical Interferometer



Michelson Interferometer
Evacuatable Cell
Interference
Beam Expander

White Light Interference
Index of Refraction
Coherence
Beam Splitter

Mach-Zehnder Interferometer
Edlen Formula
Wavelength of Light
Translucent Image Screen



In 1881 Albert Michelson used an interferometer to successfully disprove the theory of a universal ether that existed till then. Later on, he determined the length of the basic meter in units of light wavelengths with this set-up. Still, the use of interferometers in performing technical length measurements only reached significance after the discovery of the laser as a coherent light source. Today, high

precision length measuring instruments have become an important tool for many areas of the machine building industry. The Michelson interferometer commonly uses one moveable mirror which is attached to the object for which a path length measurement on nm scale is performed. The Mach-Zehnder interferometer has no moving parts and the operation is based on the retardation of one beam with respect to the other beam by changes of the index of refraction of the

probe medium. This experiment provides both, a Michelson and a Mach-Zehnder interferometer. The Michelson interferometer is used to demonstrate the classical interference patterns. For the Mach-Zehnder interferometer an evacuatable tube is inserted into one of the beam paths and the interference pattern visualizes the changes of the index of refraction. The measurement of the index of refraction of air as a function of the pressure is made by using the vacuum pump.

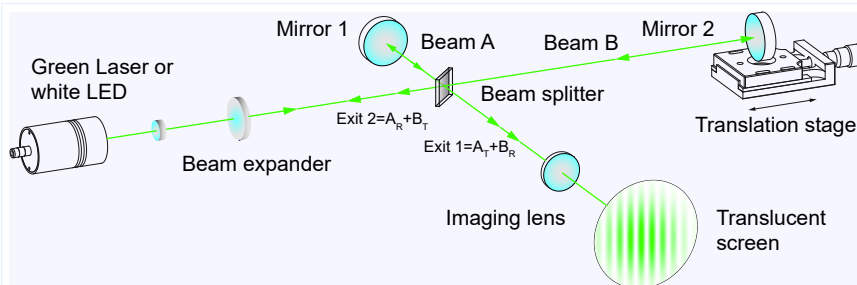


Fig. 4.29: Michelson Interferometer

The classical Michelson setup consists of the beam splitter, the mirror 1 and the mirror 2. The incident beam from either a green laser or a white light LED is split into two beams at the beam splitter. The returning beams from mirror 1 and 2 are imaged by means of a diverging lens onto a translucent screen. Mirror 2 is mounted on a translation stage for precise change of the related optical path, particularly for white light interference. The beam expander provides an enlarged beam with plane wave fronts resulting in a fringe pattern with a parallel structure. Circular rings are obtained, when the beam expander is aligned for curved wave fronts.

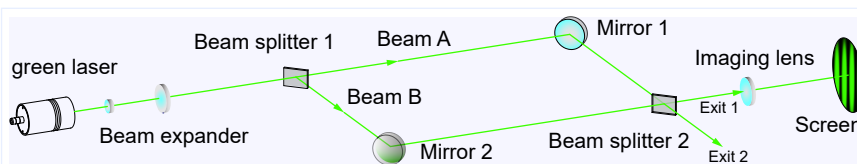


Fig. 4.30: Mach-Zehnder Interferometer

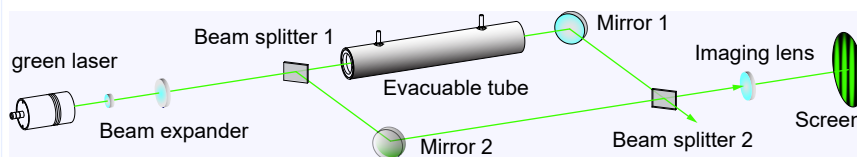


Fig. 4.31: Measuring the index of refraction as function of the pressure

The great advantage of a Mach-Zehnder interferometer lies in the fact that there are no back reflections from the interferometer mirror into the light source as it is the case with a Michelson interferometer. The back reflections create undesired fluctuations and frequency hopping of the laser. That is one of the reasons why the Mach-Zehnder Interferometer found

much more application than the Michelson setup. The beam of the green laser is enlarged by a beam expander. At beam splitter (1) the expanded beam is split into two beams (A, B) with same intensity. One propagates to the mirror (1) and the other one is deflected by 90° and travels to the mirror (2). Both beams are combined again at beam splitter (2). 50% of each beam

is transmitted and reflected. The interference pattern on the screen is created by the reflected part of A_r and the transmitted part of B_t at exit (1). At exit (2) a combination of A_r and B_r is available, however not used here. The bright to dark transitions of the interference pattern are proportional to the path or phase difference of beam A and B. In case of the Michelson, the path difference can be created by moving one of the mirrors, which is not possible with the Mach-Zehnder setup. Another way to introduce such a phase shift is to insert an optical transparent material in one arm of the interferometer and to change its index of refraction. Within this experiment a tube is used, which is filled by the surrounding air and can be evacuated. By counting the number ΔN of moved fringes for an pressure interval ΔP provides the information to calculate the index of refraction of air as function of the pressure. Additional sensors for temperature and humidity enables the comparison of the measured value for the index of refraction of air n with the results of the Edlen formula $n(P,T,H)$, whereby P is the pressure, T the temperature and H the relative humidity.

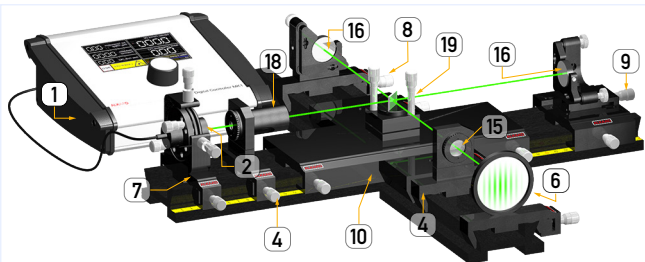


Fig. 4.32: Michelson Interferometer

A selected green laser (2) with high coherence is mounted into the adjustment holder (7). A beam expander (18) is used to enlarge the beam diameter as well as to provide plane waves. The adjustable beam splitter unit (19) splits the beam into two beams. After being reflected from the mirror (16) they are recombined by the same beam splitter. By means of the imaging lens (15) the interference pattern is imaged onto the translucent white screen (6) photographs can be taken by a standard smartphone camera. Both mirrors are mounted into precise adjustment holder to align the beams for best contrast. One mirror is mounted onto a translation stage (9). One turn of the screw moves the mirror 250 micro metre accordingly resulting in the shift of the interference pattern.

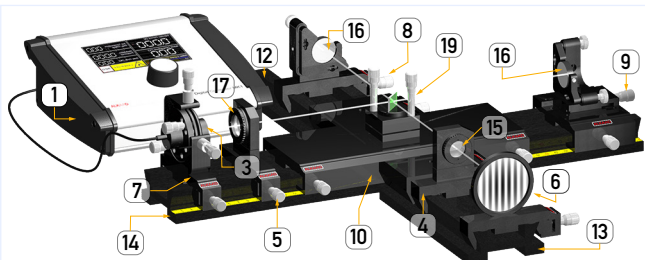


Fig. 4.33: White Light Interferometer

White light interference takes place only if the optical length of both interferometer arms have precisely the same optical length. To demonstrate

this phenomenon, a white LED (3) is used. The light of the LED is collimated by an achromat (17) inserted into the mounting plate (5). By using a ruler the initial equal distance of the mirror is aligned. For the fine tuning the translation stage (9) is used. The translation stage has a travel range of 5 mm. However, to find and hold the proper position requires patience and experience. To find the right position in an easier way the optional photodetector (22) and the audio fringe detector (23) are recommended. The fringe detector contains an AC amplifier connected to a speaker. The input is the photodetector signal. In case interference occurs a burst of tones become audible. Turning back and forth of the adjustment screw of the translation stage and listening to the bursts the proper setting can be found. In the event of such a burst of interference fringes appear and a fine tuning for best contrast may then be started.

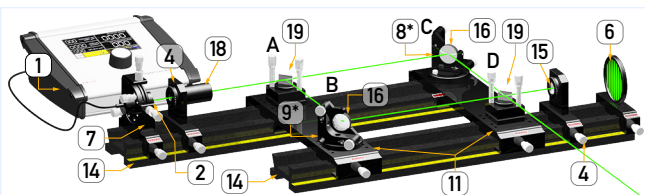


Fig. 4.34: Mach-Zehnder Interferometer

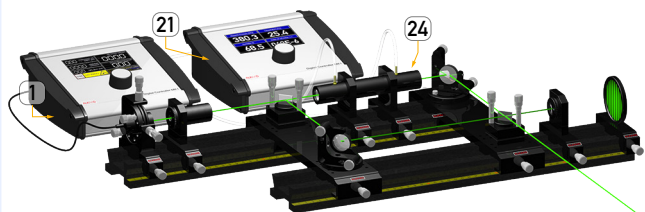


Fig. 4.35: Mach-Zehnder Interferometer with evacuable cell

Most parts of the Michelson interferometer are reused. Two bridge carrier (11) interlink two optical rails (14). The beam of the green laser (2) passes a beam expander (18) to increase the beam diameter and to provide

plane waves. Subsequently the beam is split with the first adjustable beam splitter (19, A) into two beams. Mainly the reflected beam can be adjusted whereby the transmitted beam remains unaffected. The direction of the transmitted beam will be aligned by the 4 axes adjustment holder (7) in such a way that the beam hits the centre of mirror (16, C). The reflected beam is aligned in such a way that it hits the centre of the mirror (16, B). With the mirror adjustment holder (8* and 9*) both mirrors are aligned such, that the beams hit the centre of the beam splitter plate (D). The transmitted beam shows up on the translucent white screen (6), whereby the reflected beam is aligned with the fine pitch screws of its adjustment holder (19, C). The goal of the alignment is to achieve the collinearly propagation of both beams, which is indicated by the appearance of a rich contrast interference pattern. Also here, the photograph of the interference pattern can be taken from the rear of the translucent screen by any digital camera. After perfectly aligning the Mach-Zehnder interferometer, the evacuable cell (24, option) is placed onto the rail as shown in Fig. 4.35. It is recommended to operate the cell using the vacuum controller (22, option). The controller contains a precise pressure sensor with an operating range of 300 - 1100 hPa with an accuracy of ± 0.1 hPa, a temperature sensor with an accuracy of ± 0.1 °C and a humidity sensor with an accuracy of $\pm 1\%$. The cell is connected via two flexible hoses to the vacuum controller (21). One hose is connected to the integrated vacuum pump

and the other one via a valve to the rear of the controller, where either the surrounding air or another provided gas streams into the cell. The pressure inside the cell is set by this valve and displayed on the controller. In addition, the temperature and humidity of the air or gas is displayed. Changing the pressure changes the index of refraction inside the cell and causes a shift of the interference fringes which needs to be counted visually. The measurement of the number of fringes as function of the pressure difference is recorded and transferred into a graph. From this, the index of refraction of air as a function of the pressure is derived and compared with the Edlen formula.

PE-0600 Optical Interferometer consisting of:

Item	Code	Qty.	Description	Details page
1	DC-0020	1	LED and Photodiode Controller	121 (2)
2	LQ-0020	1	Green (532 nm) DPSSL in $\varnothing 25$ housing	119 (1)
3	LQ-0200	1	White LED in $\varnothing 25$ Housing	119 (6)
4	MM-0020	2	Mounting plate C25 on carrier MG20	93 (1)
5	MM-0030	1	Mounting plate C30 on carrier MG20	93 (4)
6	MM-0110	1	Translucent screen on carrier MG20	94 (10)
7	MM-0420	1	Four axes kinematic mount on carrier MG20	96 (25)
8	MM-0440	1	Kinematic mount $\varnothing 25.4$ mm on MG20	96 (26)
9	MM-0444	1	Kinematic mount 1", translation stage on MG65	96 (28)
10	MP-0065	1	Carrier cross piece MG-65	92 (2)
11	MP-0082	2	Bridge connector for two rails plus riser plate	92 (3)
12	MP-0120	1	Optical bench MG-65, 200 mm	92 (6)
13	MP-0130	1	Optical Bench MG-65, 300 mm	93 (7)
14	MP-0150	2	Optical Bench MG-65, 500 mm	93 (8)
15	OC-0010	1	Biconcave lens $f=-10$ mm, C25 mount	98 (2)
16	OC-0100	2	Front face mirror in C25 mount	99 (7)
17	OC-0140	1	Achromat $f=40$ mm in C30 mount	99 (9)
18	OC-0320	1	Beam expander x2.7 in $\varnothing 25$ housing	100 (16)
19	OM-0010	2	Adjustable beam splitter	110 (2)
20	UM-PE06	1	Manual "Optical Interferometer"	
Option (order separately)				
21	DC-0110	1	Vacuum Controller	123 (14)
22	DC-0120	1	Si-PIN Photodetector, BPX61 with connection leads	123 (15)
23	DC-0260	1	Audio fringe detector	124 (25)
24	OM-0820	1	Gas cuvette assembly	116 (42)

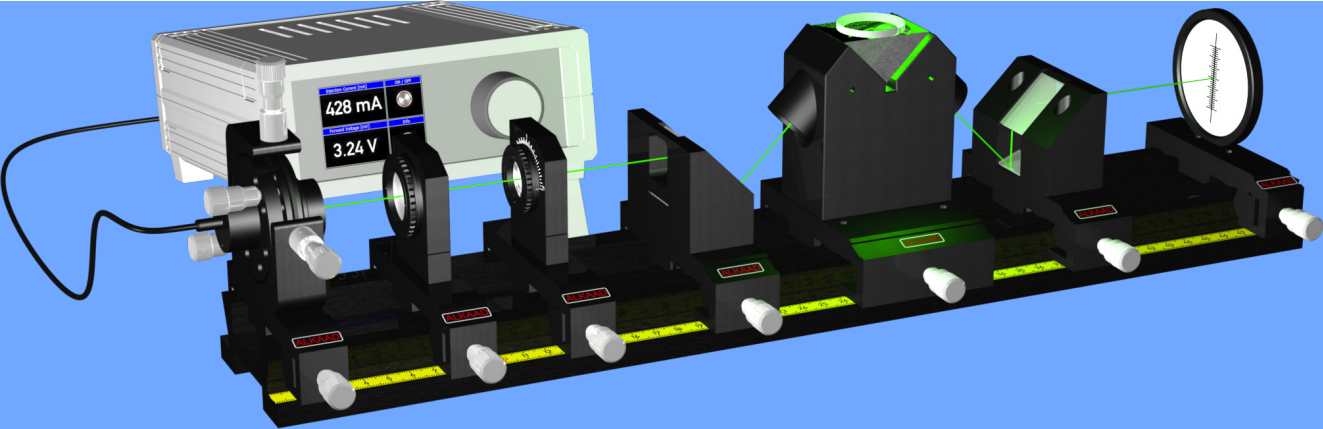
Highlights

Basic / advanced experiment


Intended institutions and users:

Physics Laboratory
Engineering department
Electronic department
Biophotonics department
Physics education in Medicine

PE-0700 Abbe Refractometer



Index of Refraction Dispersion LED Beam Forming	Prism Shadow Line Polarizer	Total Reflection LED Light Source Refractometer
---	-----------------------------------	---

 Ernst Abbe was not the first and not the only scientist who developed a convenient refractometer, but his refractometer is – in several varied and updated versions – the most widespread and most common refractometer nowadays. Although the refractometer have been replaced at the beginning of the 20th century by more specialised spectroscopic methods, it is still an important instrument for

the purity control of liquids. Consequently the Abbe refractometer developed from a laboratory instrument in basic research to an indispensable monitoring tool in industry. This experiment utilises an Abbe type refractometer. As light source a green LED is used for best eye sensitivity. Before the invention of LED, the standard yellow line of Sodium has been used. Due to the manifold of available wavelengths of the LED, ranging from UV to

IR, many tasks can be performed in industrial manufacturing, chemistry and food industry. When placing drops of a test liquid on top of the prisms the shadow line of the light beam on the screen is shifted. From this value and the device parameter the index of refraction is calculated. Liquids with known different index of refraction are provided.

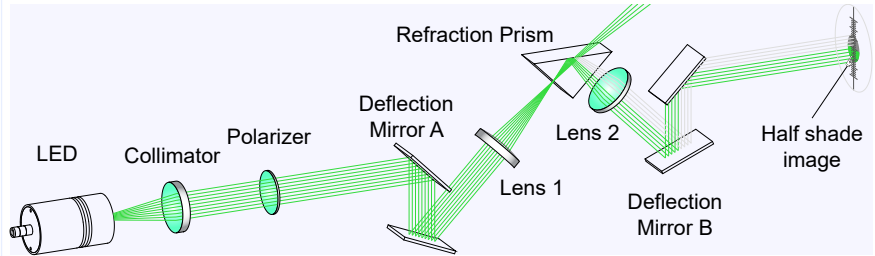


Fig. 4.36: Refractometer setup

The light of the green LED is collimated, polarized and guided by the deflection mirror (A) to the refraction prism via the lens (2). The lens (2)

creates a divergent beam in such a way that the hypotenuse of the prism is illuminated under different angles of incidence. All rays having

an angle of incidence greater than the critical angle of total reflection are leaving the prism, whereas the other are deflected and imaged via the lens (2) and the deflection mirror (B) to the translucent screen. Since parts of the beam are cut off, the initial round beam shows a clear dark area. The critical angle of total reflection depends on the index of refraction outside the prism. If a liquid or other optical transparent material is applied to the hypotenuse of the prism, this angle changes and with it the position of the dark / bright line of the half shade image, allowing the determination of the index of refraction of the applied material.

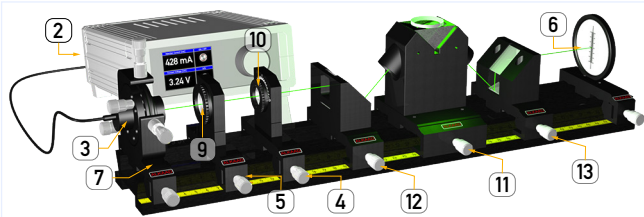


Fig. 4.37: Description of the components

The green emitting LED (3) is connected to the adaptive controller (2) which recognizes the type of the LED and automatically sets the operation limits accordingly. The emitted light is collimated by the achromat (9) to an almost parallel beam. The polarizer (10) is used to improve the contrast of the dark-bright line of the half shade image. The deflection mirror assembly (12) guides the light into the refraction prism assembly. It contains a lens to create divergent light. Another lens images the beam via the deflection mirror assembly(13) to the translucent screen (6). The test liquid (1) is applied to the top of the refraction prism. A ring shaped wall prevents spilling and can be removed for cleaning.

PE-0700 Abbe Refractometer consisting of:				
Item	Code	Qty.	Description	Details page
1	CA-0010	1	Set of test liquids	126 (2)
2	DC-0020	1	LED and Photodiode Controller	121 (2)
3	LQ-0220	1	Green LED in ø C25 housing	120 (10)
4	MM-0028	1	Mounting plate C25-S with angle gradation	93 (3)
5	MM-0030	1	Mounting plate C30 on carrier MG20	93 (4)
6	MM-0110	1	Translucent screen on carrier MG20	94 (10)
7	MM-0420	1	Four axes kinematic mount on carrier MG20	96 (25)
8	MP-0150	1	Optical Bench MG-65, 500 mm	93 (8)
9	OC-0140	1	Achromat f=40 mm in C30 mount	99 (9)
10	OC-0710	1	Polarizer in C25 mount	99 (13)
11	OM-0460	1	Refraction prism assembly	112 (18)
12	OM-0462	1	Deflection mirror unit, left	113 (19)
13	OM-0464	1	Deflection mirror unit, right	113 (20)
14	UM-PE07	1	Manual Abbe Refractometer	

 **Highlights**

Basic experiment

Intended institutions and users:

Physics Laboratory

Engineering department

Electronic department

Biophotonics department

Physics education in Medicine

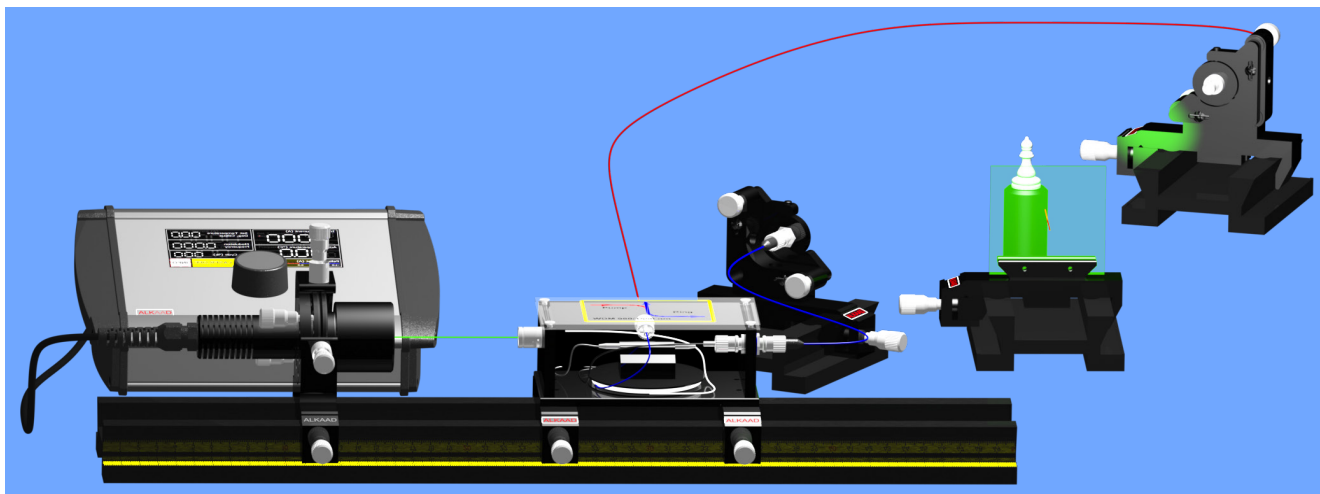
Keywords

Introduction

How it works

Optics Experiments

PE-0800 Holography



**Transmission Hologram
Interference
Single Mode Laser**

**Reflection Hologram
Fibre Spatial Filter**

**Photographic Development
Fibre Beam Splitter**

Keywords

Introduction



In 1948 – before the era of lasers – Denis Gabor developed the transmission holography technique and took the first real holograms. For the invention of holography Gabor received the Nobel Prize in 1971. In 1962 Yury Nikolayevich Denisyuk developed a holography technique which allowed to observe holograms with a white light source rather than a

monochromatic one, defined as reflection holography. Although holography did not reach the expected practical breakthrough, it is still worth to pay attention to this fascinating technique.

The experimental set-up comprises a highly coherent green laser light source and the necessary optical components to create the expanded reference and object beam. Since a green laser

source is utilised, appropriate film plates and developer are provided. Besides the optical components all required tools and materials are provided to make the developer and bleaching liquids out of provided dry chemicals. For the development of the exposed film plates all paraphernalia are provided.

How it works

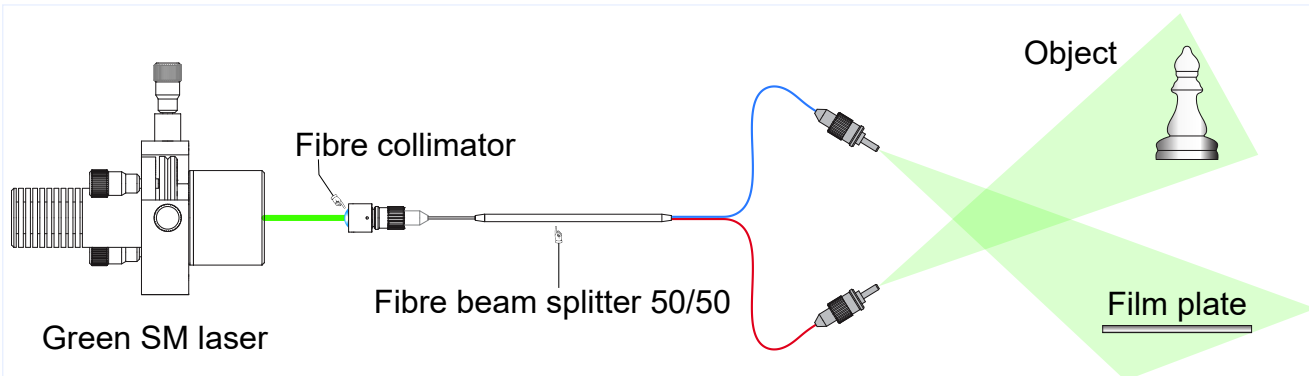


Fig. 4.38: Principle of holography setup using optical fibre

The green emission of the actively stabilized single mode laser is fed via a fibre collimator into the pig tailed fibre beam splitter creating two beams with same intensity. Each beam is guided in a single mode fibre to preserve the phase and coherence. One of the beams is directed to the object and the other to the film plate as reference beam. This unique arrangement of using modern fibre technology reduces significantly the extensive alignment of clas-

sical setups with spatial filter, separate beam splitter, expansion lens and beam bending mirrors. The optical fibre serves simultaneously as spatial filter, beam splitter and expansion lens. The only remaining adjustment is to direct the green laser radiation into the fibre, whereby the fibre collimator acts as a kind of a funnel. The precise 4 axes adjustment fine pitch screws provide a smooth and repetitious accuracy for an easy alignment process. The fibres coming

from the beam splitter are terminated with ST fibre connectors and are connected to adjustment holder for precise and sustainable alignment to either the object or the film plate. This arrangement allows the convenient direction of the light beams without affecting the initial alignment and is not restricted to a mechanical structure. Thus all kind of holography types and object illumination can freely arranged.

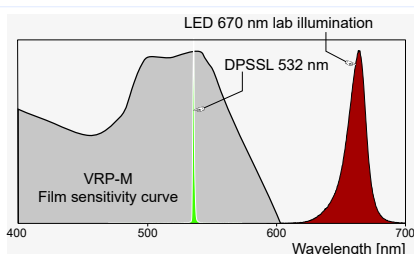
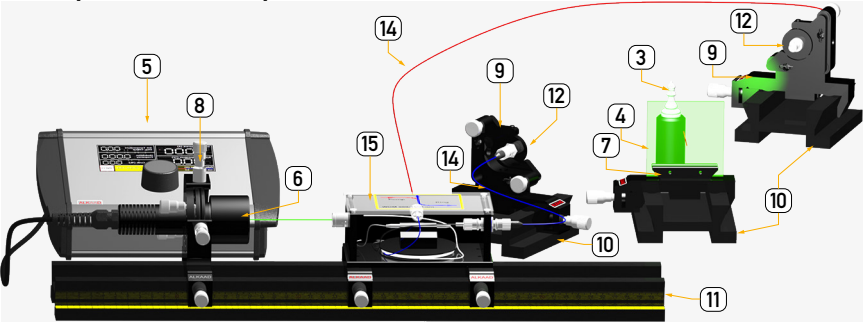


Fig. 4.39: Sensitivity of the VRP-M film

The availability of powerful single mode laser emitting in the green spectral range (532 nm) led to the development of holographic films with adapted sensitivity (Fig. 4.39). The classical holography setup used red light as provided by the HeNe laser, requiring film plates with sensitivity in this spectral range. However, the output power of HeNe reached for large systems around 50 mW, whereas the small DPSSL can reach several watts of green radiation. In this setup we are using a green laser with 50 mW

resulting in exposure times of several seconds only, whereas HeNe laser based setups require considerable longer exposure times. It is obvious, that long exposure times require a much more stable structures and vice versa. The sensitivity of the VRP-M drops beyond 600 nm to zero. This allows the use of deep red (670 nm) LED lamps to illuminate the holography work place without affecting the film plate.

Description of the components



The temperature and injection current of the laser (6) is actively stabilized by the controller (5) and serves also as timer for the exposure. The laser light is coupled into the beam splitter unit (15) and distributed with a splitting ratio of 50/50% into the two fibre (14). Each fibre is terminated with a ST fibre connector which are connected to the panel jack insert (12) of the adjustment holder (9). The two adjustment holders for the fibre and the plate holder (7) are placed onto a 100 mm long optical bench (10) to achieve the required stability. All components can be arranged freely to each other to find the best illumination of the target (3) and the film plate which is held by the spring loaded filter plate holder (7).



Fig. 4.40: Set of dry chemicals (2)



Fig. 4.41: Development equipment (1): Balance, beaker, stirring staff and scoop (left) and (right) 3 lab dishes, 3 wide mouth bottles and 3 film tongs



Fig. 4.42: Transmission hologram sample

The experiment comes with a ready made professional transmission hologram of chess pieces (Fig. 4.42) which is illuminated by one of the two expanded beams and the hologram becomes visible. However, to make the own hologram requires the weighing and mixing of the dry development and bleaching chemicals. A precise step by step instruction is given in the manual (16). The set of dry chemicals (2) are good for 4 litres of developer and bleaching liquid. The chemicals are used are standard and available in good lab equipment shops. The experiment comes with a lightproof box containing 30 film plates (4) with a size of 63x63 mm.



Fig. 4.43: Holographic film plates

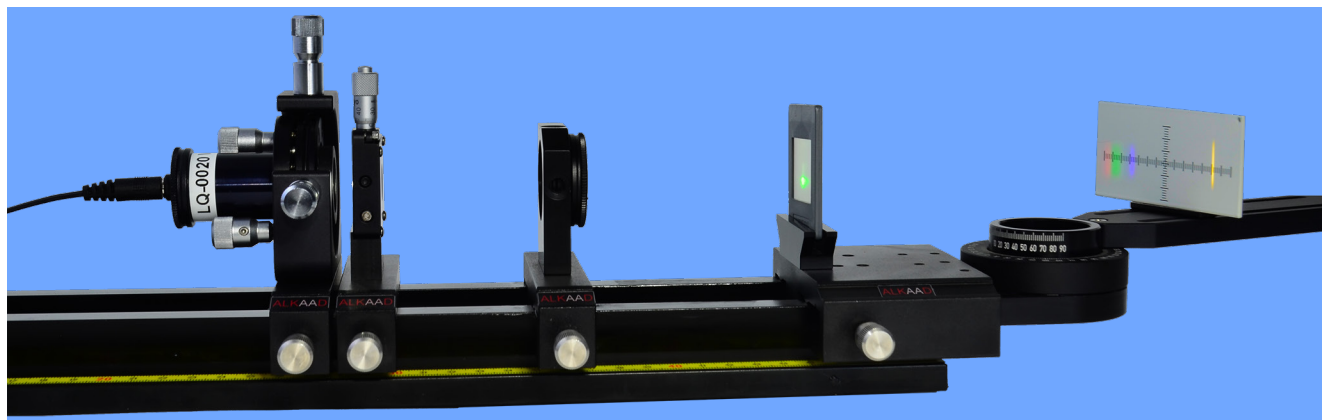
PE-0800 Holography consisting of:

Item	Code	Qty.	Description	Details page
1	CA-0030	1	Set of development equipment	126 (4)
2	CA-0034	1	Set of developer chemicals	127 (5)
3	CA-0036	1	Sample object for holography	127 (6)
4	CA-0038	30	Photographic plate VRP-M, 532 nm, 63 x 63 mm	127 (7)
5	DC-0090	1	Laser controller & exposition timer	123 (12)
6	LQ-0040	1	Green (532 nm) stabilized Laser, 40 mW	119 (3)
7	MM-0060	1	Filter plate holder on MG20	94 (7)
8	MM-0420	1	Four axes kinematic mount on carrier MG20	96 (25)
9	MM-0440	2	Kinematic mount ø25.4 mm on MG20	96 (25)
10	MP-0110	3	Optical Bench MG-65, 100 mm	92 (5)
11	MP-0150	1	Optical Bench MG-65, 500 mm	93 (8)
12	OC-0430	2	Fibre jacket in C25 mount	100 (21)
13	OC-0490	1	Sample transmission hologram (chess pieces)	101 (28)
14	OC-2020	2	ST/ST SM Fibre patch cable, length 1 m	108 (92)
15	OC-2360	1	Fibre SM beam splitter unit	109 (95)
16	UM-PE08	1	Manual Holography	
Option (order separately)				
17	LQ-0214	1	Dark Red LED in ø 25 housing	120 (9)

Highlights

Basic experiment ★★ ★
High level of fascination
Intended institutions and users:
Physics Laboratory
Engineering department
Electronic department
Biophotonics department
Physics education in Medicine

PE-0900 Diffraction Grating



Keywords

Grating Constant
Reflection Grating
Diffraction Order

Amplitude Grating
Transmission Grating

Phase Grating,
Spectral Resolution

Introduction

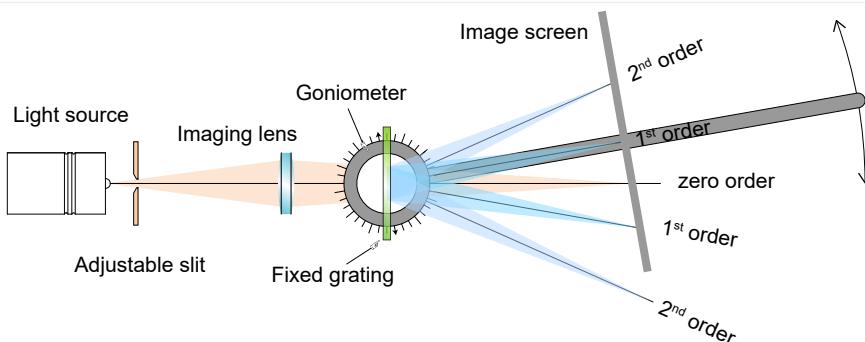


Joseph von Fraunhofer, the investigator of the solar lines, invented the diffraction grating in 1821. This optical element showed a much higher dispersion than any glass prism and allowed Fraunhofer to investigate the solar spectrum in a resolution much better than ever seen before. Enormous quality improvement as well as optimization of the manufacturing technique of ruled gratings are

the results of Henry Rowlands efforts in development of diffraction gratings. His gratings were used worldwide and were unbeaten in quality and resolution for decades. Nowadays holographic techniques using the interference of laser beams allow manufacturing gratings with larger grating constants and bigger size. The experiment comprises transmission gratings of different grating constants (lines per cm) a green laser with known wavelength of 532 nm

and a white LED lamp emitting a variety of different spectral lines. The resulting interference pattern is imaged on a white screen with mm scale to measure the angle of the emitted light. Applying gratings with different parameter the resolution power is demonstrated. By using a mesh like two-dimensional grating impressive patterns of light spots are created and the analogy to the principles of x-ray diffraction on crystal lattices or atomic layers demonstrated.

How it works



The emitted radiation of the light source illuminates the adjustable slit. The image of the slit is projected by means of the imaging lens to the image screen which is fixed to the goniometer arm. After passing the grating the incident light is divided into multiple orders and the spectral distribution becomes visible as vertical bars (line), the image of the slit. The intensity of the image on the screen depends on the adjusted width of the slit. Closely neighboured lines may merge if the width of the slit is too wide. At this point the resolution comes into consideration and other gratings (1) with different grating constants are applied.

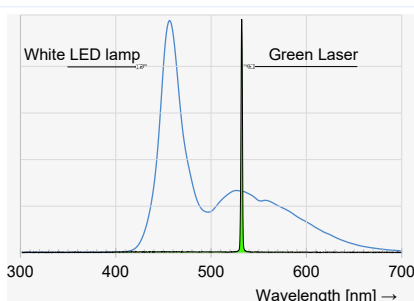


Fig. 4.44: Spectral distribution of the used light sources



Fig. 4.45: Spectral distribution of the white LED seen behind the grating

Two different light sources are used. One is a green emitting laser (2) with a very narrow spectral distribution and the other one a white light LED (3) which emits a broad spectrum as shown in Fig. 4.44. A white and translucent screen () is provided to take impressive photographs of the created diffraction pattern. Fig. 4.45 shows such a photograph. In the centre the zero order appears and symmetrical to it the $\pm 1^{\text{st}}$ order. Moving the screen closer to the grating also the 2nd order appears, however, with much lower intensity. The green laser is used as wavelength reference (532 nm) to calibrate the setup for quantitative measurements.

PE-0900 Diffraction Grating consisting of:

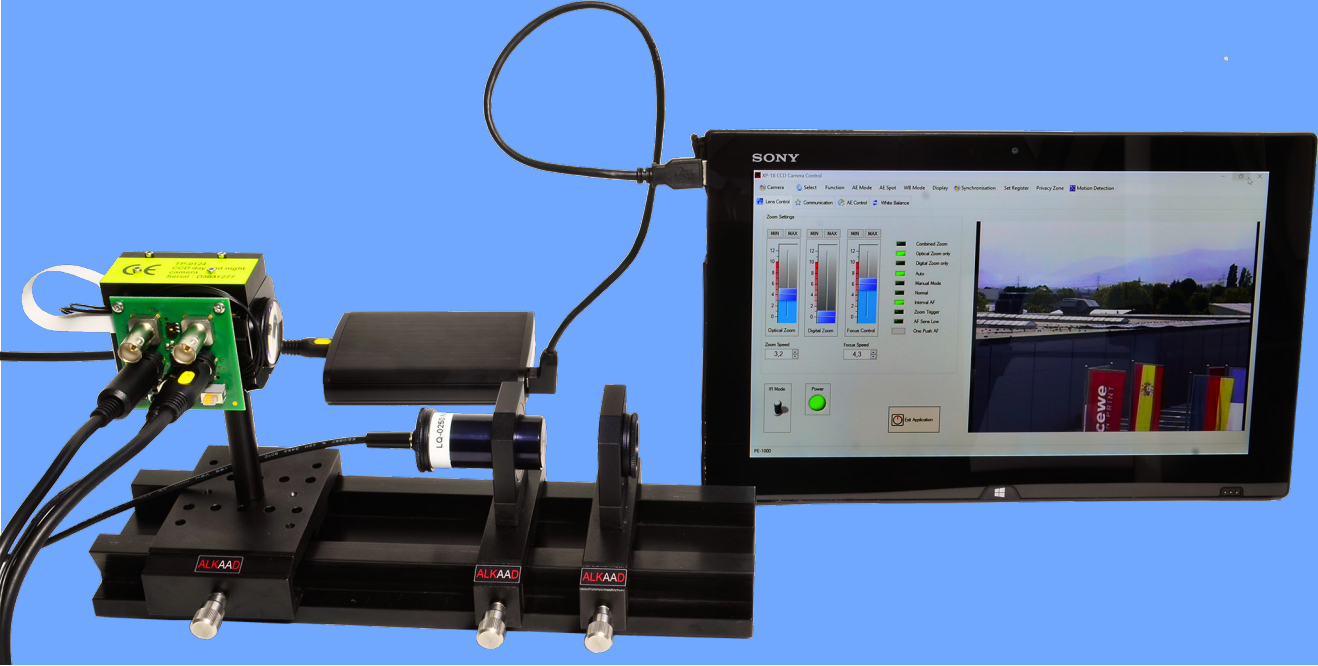
Item	Code	Qty.	Description	Details page
1	CA-0040	1	Set of 5 transmission gratings	127 (8)
2	LQ-0020	1	Green (532 nm) DPSSL in $\varnothing 25$ housing	119 (1)
3	LQ-0200	1	White LED in $\varnothing 25$ Housing	119 (6)
4	MM-0032	1	Mounting plate C30-V on carrier MG20	93 (5)
5	MM-0110	1	Translucent screen on carrier MG20	94 (10)
6	MM-0300	1	Carrier with 360° rotary arm	95 (20)
7	MM-0420	1	Four axes kinematic mount on carrier MG20	96 (25)
8	MP-0150	1	Optical Bench MG-65, 500 mm	93 (8)
9	MP-0220	1	White screen with XY scale on block	93 (9)
10	OC-0140	1	Achromat f=40 mm in C30 mount	99 (9)
11	UM-PE09	1	Manual Diffraction Grating	




Highlights

Basic experiment
Impressive images
Intended institutions and users:
Physics Laboratory
Engineering department
Electronic department
Biophotonics department
Physics education in Medicine

PE-1000 Camera and Imaging

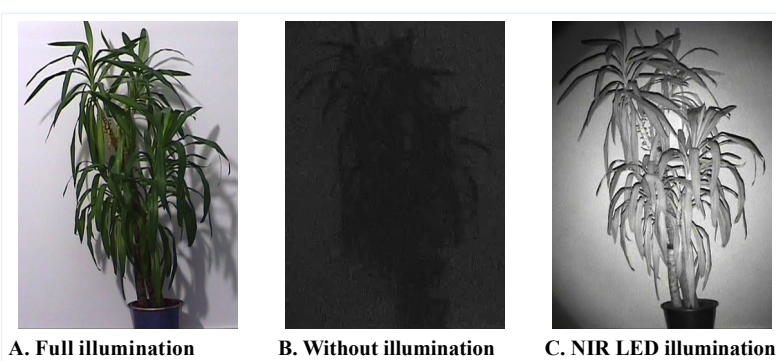


Pinhole Camera CCD Sensor Spectral Sensitivity of CCD Chip	Camera Obscura Magnification Active Night Vision	Objective Iris and Depth of Field
---	---	--

 The principle of creating an image through projection on a surface is known since ancient times. Aristotle observed images of the sun through holes generated by the leaves of a tree, while Arab scientists used this principle in astronomy to observe the solar eclipses. The clearest and detailed description is made by Leonardo da Vinci in his work “Codice Atlantico” where for the first time, the structure of the human eye is commented as a “camera obscura”. But most of our respect should be paid to

Giovanni Antonio Canaletto. As a painter he used the principle of the camera obscura in a very practical and commercial application. Although he did not take photographs as one understands it today, he imaged scenes and objects on canvas through a narrow hole in a curtain and painted them. With the help of this technique he was able to produce more than 900 paintings during his period. Later Giovanni Battista Della Porta suggested for the first time that a lens may be applied to the hole. This was the initial step for the invention of the portable “camera obscura” as a working tool for

outlining at that time. In the frame of this experiment a high performance industrial CCD zoom camera with USB computer connection is applied. Parameters like diaphragm size, position and the influence of lenses on the brightness, sharpness and dimensions of the image are investigated. The variable diaphragm demonstrates the effect of depth of field. Furthermore a LED emitting invisible radiation to the human eye is provided to study the exciting technology of active night vision.



A. Full illumination B. Without illumination C. NIR LED illumination

The series of pictures taken with the CCD camera shows an example (A) at full illumination and (B) in the darkened room. Due to high sensitivity of the camera a dimly shape of the object can be seen. In that moment, when the NIR LED is switched on and the camera switched into the NIR mode, a bright black and white image of the object appears. The leaves of the plant appear in white colour, indicating the reflection of the NIR radiation. To document the recorded images the frame grabber and the note pad is used. For each measurement with different parameters like the iris diameter, focusing, exposition time and so on a file for the students report is created.

PE-1000 CCD Camera & Night Vision consisting of:				
Item	Code	Qty.	Description	Details page
1	CA-0110	1	CCD day & night camera block module	128 (14)
2	CA-0120	1	Tablet PC Windows	128 (15)
3	CA-0150	1	USB Video frame grabber	129 (18)
4	ES-1000	1	Camera control software	
5	LQ-0250	1	NIR LED in ø 25 housing	120 (13)
6	MM-0020	2	Mounting plate C25 on carrier MG20	93 (1)
7	MP-0130	1	Optical Bench MG-65, 300 mm	93 (7)
8	OC-0060	1	Biconvex lens f=60 mm in C25 mount	99 (5)
9	UM-PE10	1	Manual Camera & Night Vision	
Option (order separately)				
10	CA-0100	1	Flat panel TV	128 (13)

 **Highlights**

Basic experiment

★ ★ ★ Night vision

Intended institutions and users:

Physics Laboratory

Engineering department

Electronic department

Biophotonics department

Physics education in Medicine

Security forces

Keywords

Introduction

How it works

Optics Experiments

PE-1100 LED and Diodelaser



Electroluminescence
Laser Diode
Spatial Intensity Distribution

Semiconductor
Monochromatic Light
Beam Shaping

LED
Coherence
Cylindrical Lenses



Nick Holonyak developed the first practical LED in 1962. When electrically biased in the forward direction, an LED is able to emit light through electroluminescence.

The colour of the emission depends on the semi conducting material used, and can be near-ultraviolet, visible or infrared. The semi conducting chip is encased in a solid plastic lens, which is much more resistant than the glass en-

velope of a traditional light bulb or tube. Most typical LEDs are designed to operate with no more than 30-60 mW of electrical power. High power devices produce light similar to a 50 watt light bulb, and facilitate the use of LEDs for general illumination needs. The typical working lifetime of an LED is ten years, which is much longer than the lifetimes of most other light sources. Robert N. Hall is usually cited as the inventor of the semiconductor laser, but

Holonyak was involved in the development as well. In laser diodes, light is generated basically on the same principle like in LEDs. But by especially designed semiconductor material laser operation is achieved rather than spontaneous luminescence. Within this experiment, the properties of LEDs and laser diodes spectral and beam characteristics are investigated and beam shaping experiments are performed.

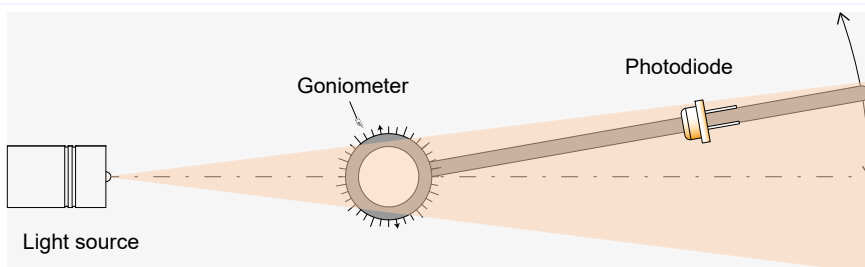


Fig. 4.49: Measuring the spatial intensity distribution

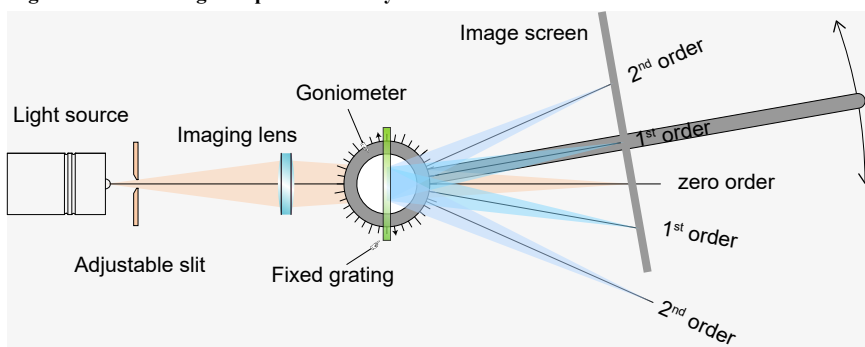


Fig. 4.50: Measuring the spectral distribution

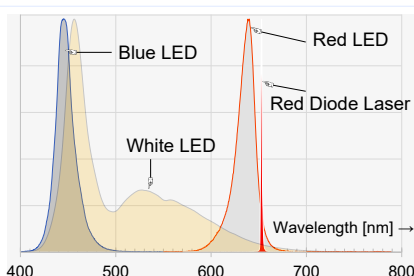


Fig. 4.46: Spectra of the used light sources



Fig. 4.47: Spectral distribution of the laser diode



Fig. 4.48: Spectral distribution of the white LED

Description of the components



Different light sources like red laser diode (4), blue LED (7), red LED and white LED (5) are inserted into the four axes adjustment holder (13). An adjustable slit on a carrier is provided to create a line which is imaged by the achromat (16) to the white screen as line. After passing the grating (19) the incident light is spread with respect to its wavelength into the first and higher order lines. With a goniometer (12) and the scale of the white screen (15) the angle of the individual lines are measured. The photodetector (2) is used to measure the angle resolved intensity distribution. The grating (19) and the white screen (15) are removed for this purpose.

Beam shaping of the diode laser

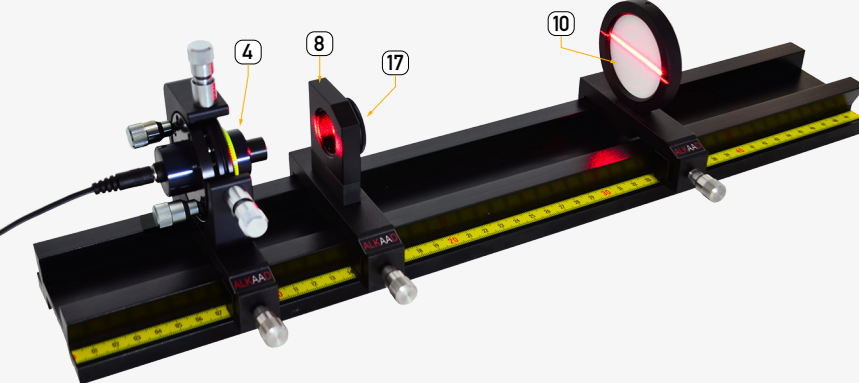


Fig. 4.51: Creating a laser line with a cylindrical lens

From the Fig. 4.51 the elliptical intensity distribution of the red laser diode (4) can be seen on the mounting plate (8). A cylindrical lens (17) treats the beam in such a way, that a horizontal or vertical line is created. The orientation of the line depends on the orientation of the cylindrical lens with respect to the beam profile of the laser diode. The created laser line is imaged to the translucent screen (10). Such laser lines are commonly used to create a straight line in building construction or found more and more as alignment aid in handheld buzz saws.

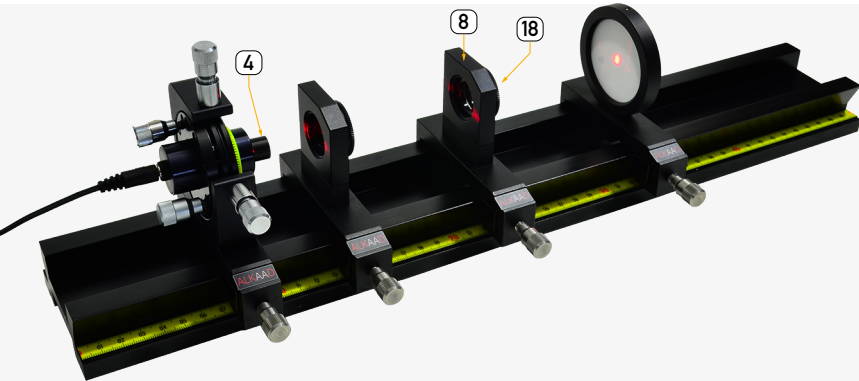


Fig. 4.52: Round beam formation with two cylindrical lenses

In this setup two cylindrical lenses are used in telescopic arrangement and serves two purposes. One of it is the formation of a round beam out of the elliptical beam profile of the laser diode as shown in Fig. 4.52. Another application is the creation of a laser line like that one of the previous experiment. However, due to the use of two cylindrical lenses an almost parallel line is generated. Using only one lens a sharp image appears only in a certain distance.

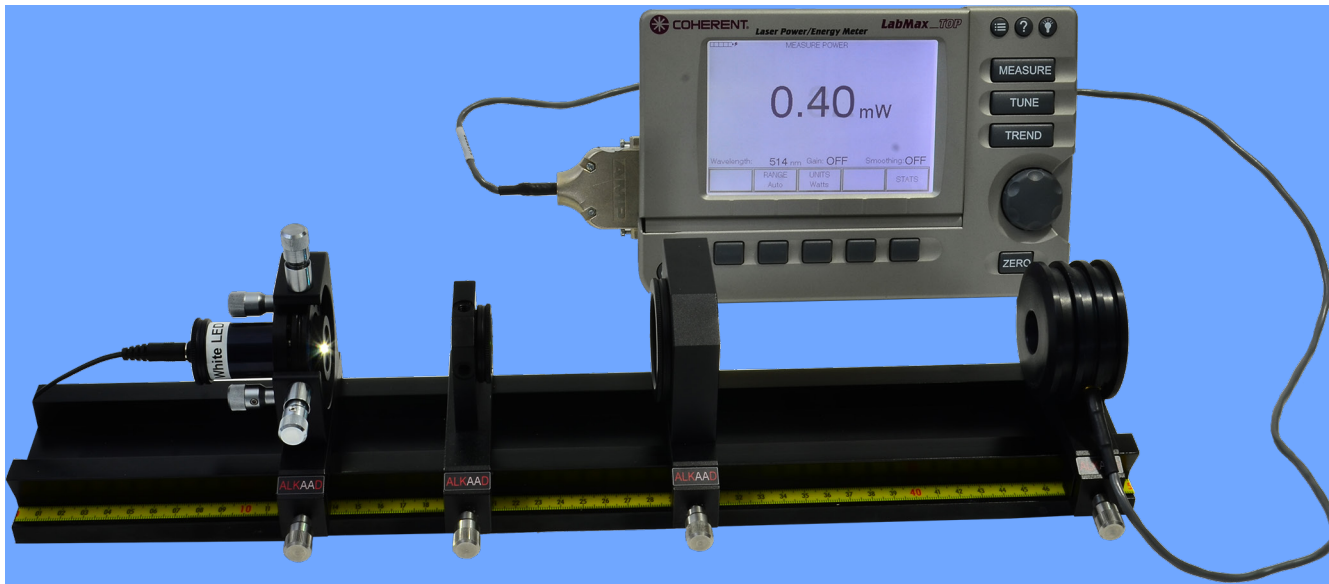
PE-1100 LED and Diodelaser consisting of:

Item	Code	Qty.	Description	Details page
1	CA-0220	1	Multimeter 3 1/2 digits	129 (21)
2	DC-0120	1	Si-PIN Photodetector, BPX61 with connection leads	123 (15)
3	DC-0380	1	Photodetector Junction Box ZBI	125 (31)
4	LQ-0060	1	Red (635 nm) diode laser in ø 25 housing	119 (4)
5	LQ-0200	1	White LED in ø 25 Housing	119 (6)
6	LQ-0210	1	Red LED in ø 25 housing	119 (7)
7	LQ-0230	1	Blue LED in ø 25 housing	120 (12)
8	MM-0020	2	Mounting plate C25 on carrier MG20	93 (1)
9	MM-0032	1	Mounting plate C30-V on carrier MG20	93 (5)
10	MM-0110	1	Translucent screen on carrier MG20	94 (10)
11	MM-0240	1	Adjustable slit om carrier 20 mm	95 (19)
12	MM-0300	1	Carrier with 360° rotary arm	95 (20)
13	MM-0450	1	XY Adjustment holder with rotary insert on MG20	96 (29)
14	MP-0150	1	Optical Bench MG-65, 500 mm	93 (8)
15	MP-0220	1	White screen with XY scale on block	93 (9)
16	OC-0140	1	Achromat f=40 mm in C30 mount	99 (9)
17	OC-0220	1	Cylindrical lens f=20 mm in C25 mount	100 (14)
18	OC-0280	1	Cylindrical lens f=80 mm in C25 mount	100 (15)
19	OC-0460	1	Transmission grating 600 l/mm	100 (22)
20	UM-PE11	1	Manual LED and Laser Diode	

Highlights

- Basic experiment
- Impressive images
- Intended institutions and users:
- Physics Laboratory
- Engineering department
- Electronic department
- Biophotonics department
- Physics education in Medicine

PE-1300 Radio-and Photometry of Light



Keywords

Black Body Radiator
V(λ) Filter
LED Light

Thermal and Cold Light
Photometric Units
Incandescent Light

Spectral Sensitivity of Human eye
Calibrated Radiometer
Energy Saver Lamp

Introduction



The values of optical radiation are usually measured in radiometric units as watt seconds or watts, however, the visible part of optical radiation has its own photometric units with a basic unit known as candela (cd). It is the sixth unit apart from the basic units length (m), mass (kg), time (s), electrical current (A) and temperature (T), which were defined during the 10th International Conference for Weights and Measures in 1954. All these units have an official measure which is standardised worldwide by calibrating institutes. The length for example, was for a long time defined by the primary standard meter in Paris, now it is defined by how long it takes light to pass through 1 meter in vacuum multiplied by the fixed speed of light in vacuum. The standards for mass, time etc. are also well known. However, the units in

light engineering are not as common to us since we do not come across the measurement in our daily lives. These units however, are indispensable for the preparation of lighting equipment for the various kinds of places people inhabit. In optical science the whole optical, spectral range of radiation is taken into consideration, which covers a wavelength range of 0.2 mm to approximately 1 mm. In light engineering or photometry however, only the range that can be perceived by the human eye is of interest. Since the sensitivity of the eye is a subjective unit, the International Commission for Lighting has defined the curve of the spectral response of the human eye $V(\lambda)$. Several measurements were taken on people to obtain a statistical result for this purpose. Photometry considers the subjective spectral response (sensitivity) of the human eye combined with strict physical

rules. The sensitivity of the human eye is the measure of all things in photometry. Within this experiment the basics of light are given in the comprehensive manual. The black body radiation is discussed in detail as well as the transition to photometric units. The key component of the experiment is the $V(\lambda)$ filter which is designed in such a way that it represents the sensitivity curve of an average human eye. The experiments come with two LED with different spectral emission, an energy saving and an incandescent lamp both having almost the same electrical power. A wavelength independent optical power meter is used to measure the power with and without $V(\lambda)$ filter. From this measurements the optical power in radiometric as well as photometric units are measured.

How it works

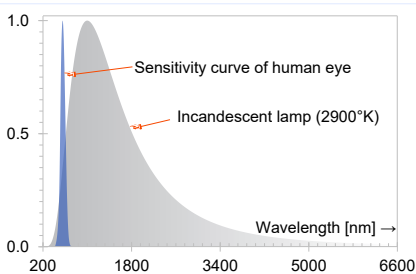


Fig. 4.53: Incandescent lamp

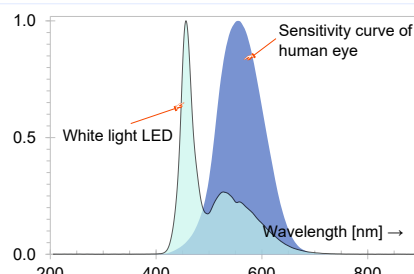


Fig. 4.54: White light LED

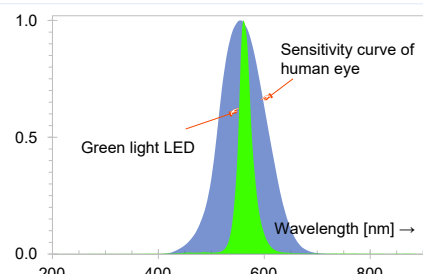


Fig. 4.55: Green light LED

PE-1300 Radio-and Photometry of Light consisting of:

Item	Code	Qty.	Description	Details page
1	CA-0260	1	Laser power meter LabMax-TO	129 (22)
2	DC-0200	1	High sensitive power sensor, 0.3-11 μ m	124 (21)
3	LQ-0200	1	White LED in ϕ 25 Housing	119 (6)
4	LQ-0220	1	Green LED in ϕ 25 housing	120 (10)
5	LQ-0410	1	Energy saving lamp GU10, 9W/230V	120 (16)
6	LQ-0450	1	Tungsten lamp, GU10, 10 W/230V	121 (18)
7	MM-0020	1	Mounting plate C25 on carrier MG20	93 (1)
8	MM-0050	2	Mounting plate C50 with carrier MG20	94 (6)
9	MM-0620	1	Lamp socket GU10 on MG65	98 (40)
10	MP-0150	1	Optical Bench MG-65, 500 mm	93 (8)
11	OC-0150	1	Biconvex lens $f=150$ mm in C50 mount	99 (10)
12	OC-0920	1	$V(\lambda)$ filter in C50 mount	104 (52)
13	UM-PE13	1	Manual Radio and Photometry	

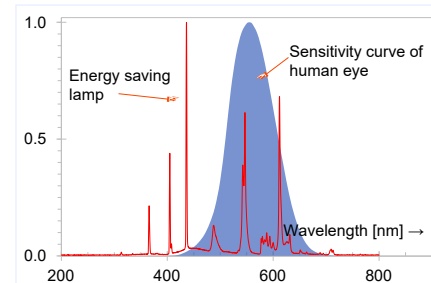
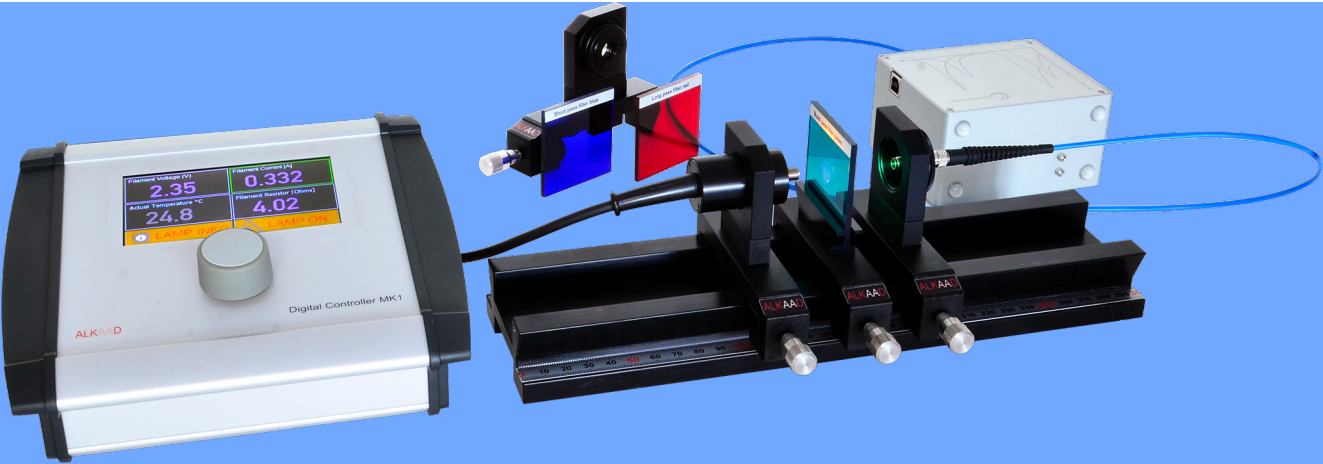


Fig. 4.56: Energy saving lamp in relation to the sensitivity curve of the human eye

PE-1400 Spectrometer

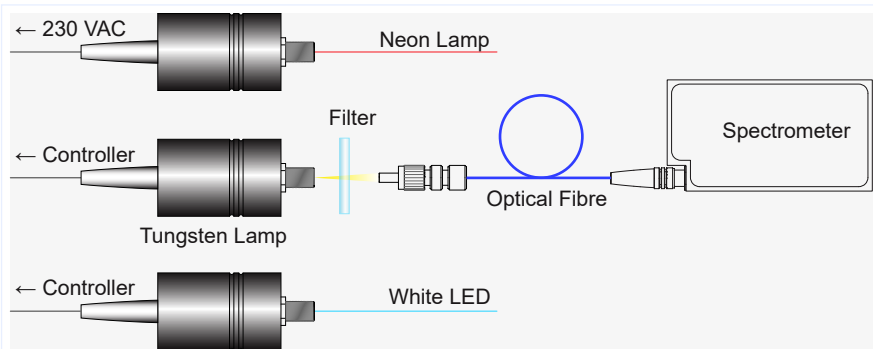


Spectrometer Incandescent Light Source Emission Spectra	Fibre Coupled Neon Spectral Lamp Transmission and Absorption Spectra	LED Light Sources Optical Filter
--	---	---

An optical spectrometer or simply spectrometer is an apparatus to record the intensity distribution as a function of the wavelength of a light source. Spectrometers played and still play an important role in a variety of applications. The emitted radiation from a source provides information about the atomic and molecular energetically structure. It is a keyhole into the fascinating world of quantum mechanical and optical processes. The first spectrometer used prisms to achieve the required spatial separation of the incom-

ing light. By using a precise goniometer the exit angle is measured and set into relation of the wavelength. The emerging optical gratings made the spectrometer more precise and enhanced the resolution significantly. Another step towards more convenient use can be seen in the development of two dimensional CCD chips allowing the real time measurement and data storage with computer. Last but not least the optical fibre made it very comfortable to bring the light to the spectrometer. Today's spectrometers are available in a size of half a brick providing a spectral range from 200

to 1200 nm with a resolution of 1 nm. Such a spectrometer is part of this experiment to train the students in the application of the most import optical measuring apparatus. Within the scope of the experiments three different light sources are used and characterised by the spectrometer. The spectra of a white light, a Neon spectral lamp and an incandescent lamp are compared and discussed. Four optical filter are placed in the front of the light sources and the transmission spectrum recorded.



The light entrance of the spectrometer is formed by the entry slit with a width designed for the intended use. It is typically 50 μm to achieve a resolution of 1 nm in a range of 200-1200 nm. Of course the resolution depends on further parameters like the internal geometry and the grating constant. The slit is located directly behind the fibre panel jack and is illuminated directly or by the attached fibre. The provided sample lamps are equipped with matching fibre jack to allow the direct connection with the fibre. To practise the important absorption measurement a set of different filters are used. Finally a Neon spectral lamp is provided which emits a number of lines with precisely known wavelength. The comparison of the spectrometer reading to this lines allows the calibration of the spectrometer.

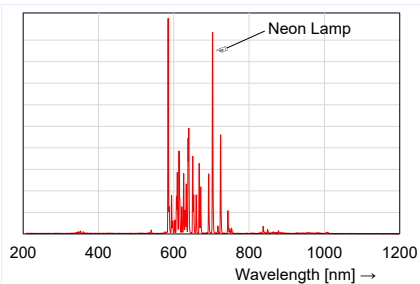


Fig. 4.57: Line spectrum of the Neon lamp with known wavelength

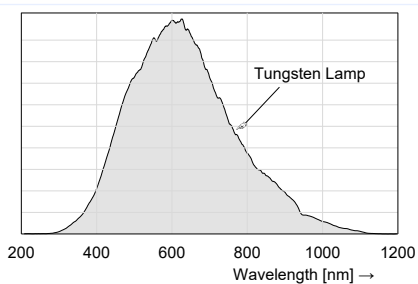


Fig. 4.58: Measured spectrum of the tungsten wire lamp

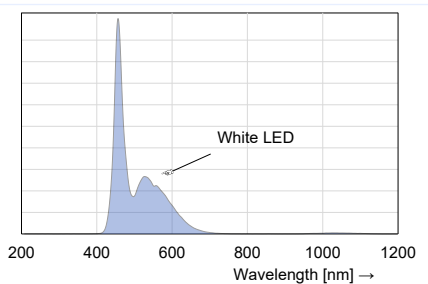


Fig. 4.59: Measured spectrum of the white light lamp

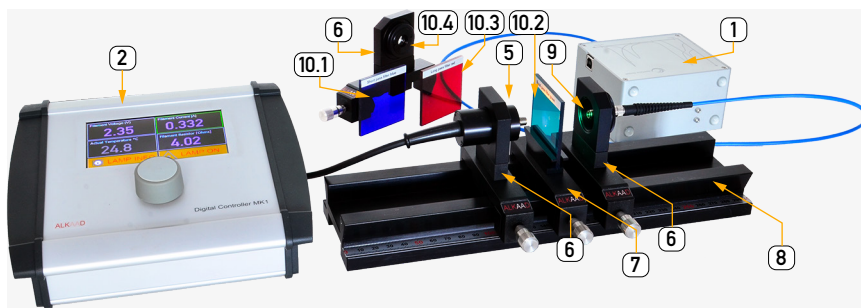
Keywords

Introduction

How it works

Optics Experiments

Description of the components



The individual sample lamps are inserted into the mounting plate (6). The precise operation

of the tungsten wire lamp requires the current controller (2). The Neon spectral lamp (3) is di-

rectly operated from the 230 VAC mains and the white light LED from the provided ordinary 5V wall plug power supply. The fibre of the spectrometer (1) is directly attached to the lamps or to the adapter (9) which is inserted into a mounting plate for free space experiments like the absorption measurements. The optical bench (8) serves as a sturdy base. Instead of the filter plate holder a mounting plate (6) with the laser line filter (10.4) can be used. The controller (2) provides and controls the current for the precision tungsten lamp (5). It allows the determination of the filament temperature and the wavelength of the maximum intensity.

Measurements

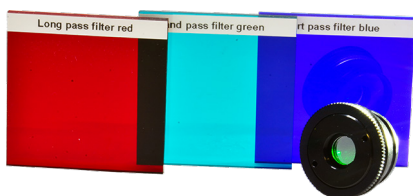


Fig. 4.60: Set of four filter (10)

The Fig. 4.60 shows the filter used in the experiment. From left to right:

filter #1, filter #2 and filter #3.

In front of the filter 3 the narrow laser line (532 nm) in a C25 mount is shown. This filter is inserted into one of the mounting plates 6, whereas the other filter are accommodated in the filter plate holder (7)

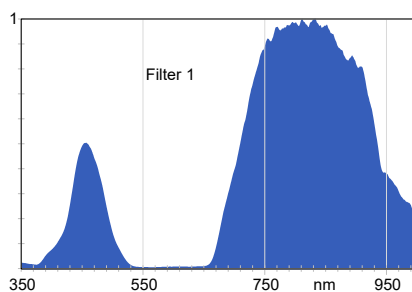


Fig. 4.61: Filter #1 transmission curve

This filter has a size of 50x50 mm and is designed to pass the blue light in the visible range and blocks the red part of the visible spectrum.

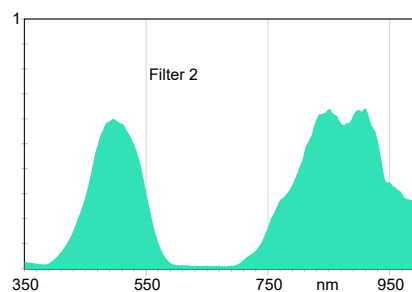


Fig. 4.62: Filter #2 transmission

The filter 2 has a size of 50x50 mm and is designed to pass the blue green and blocks the red part of the visible spectrum

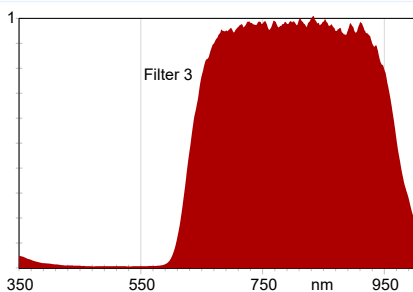


Fig. 4.63: Filter #3 transmission curve

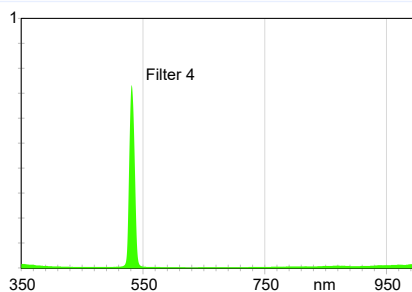


Fig. 4.64: Laser line Filter #4

The filter #3 is named as red long pass filter because it passes the red and near infrared part of the spectrum and blocks the range below 600 nm. A totally different behaviour is shown by the filter #4 which is a so called interference or laser line filter. The designed behaviour is achieved by coating a glass plate with different layers. Such a filter is useful in spectroscopy in a narrow spectral range without distortion of undesired light. The filter is mounted into a C25 holder (see Fig. 4.60) and can be inserted into a mounting plate (6).

PE-1400 Spectrometer consisting of:

Item	Code	Qty.	Description	Details page
1	CA-0270	1	Fibre coupled spectrometer 200 - 1200 nm, USB	130 (26)
2	DC-0270	1	Filament and LED lamp controller	125 (26)
3	LQ-0100	1	Neon spectral lamp	119 (5)
4	LQ-0200	1	White LED in ø 25 Housing	119 (1)
5	LQ-0440	1	Tungsten filament white light source	121 (17)
6	MM-0020	3	Mounting plate C25 on carrier MG20	93 (1)
7	MM-0060	1	Filter plate holder on MG20	94 (6)
8	MP-0130	1	Optical Bench MG-65, 300 mm	93 (7)
9	OC-0430	1	Fibre jacket in C25 mount	100 (21)
10	OM-0200	1	Set of 4 optical filter	111 (10)
11	UM-PE14	1	Manual Spectrometer	



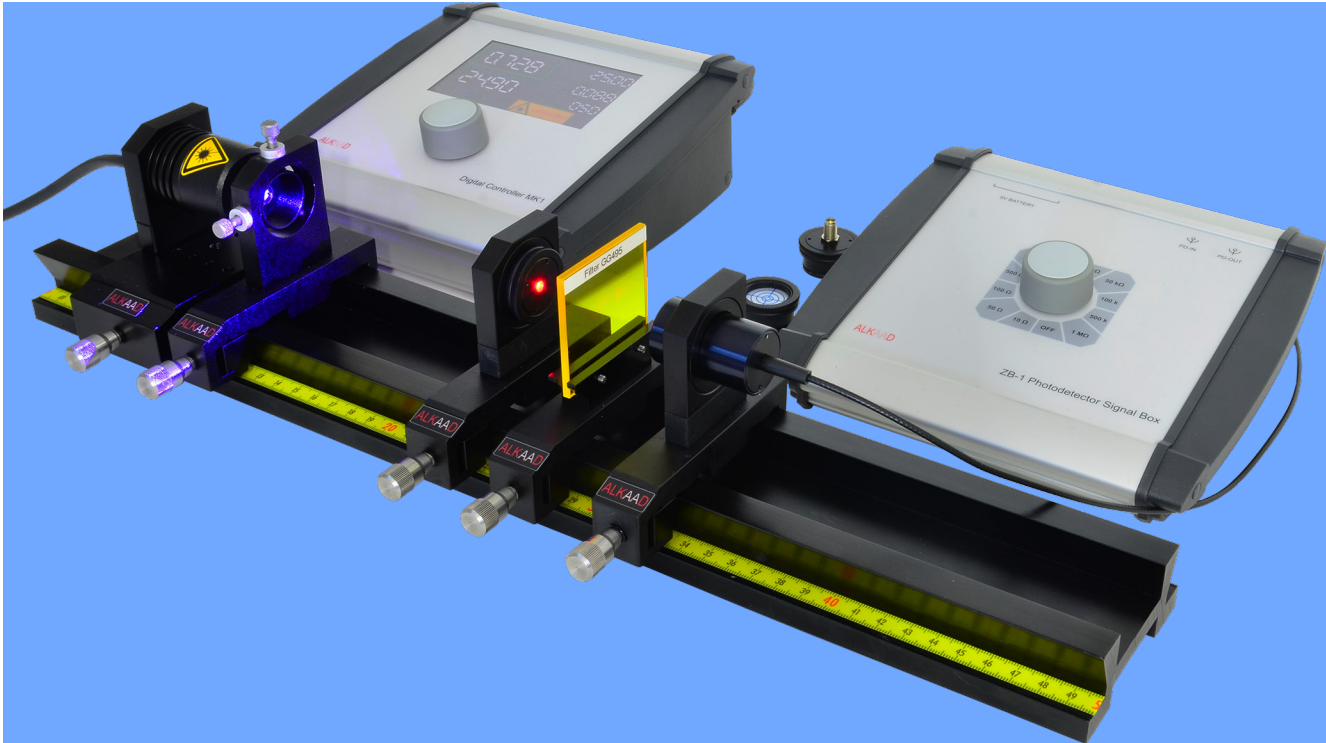
Highlights

Basic experiment


Intended institutions and users:

Physics Laboratory
Chemistry Laboratory
Engineering department
Electronic department
Biophotonics department
Physics education in Medicine

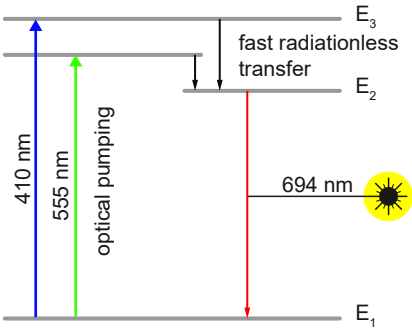
PE-1500 Ruby Excited Lifetime & Spectroscopy



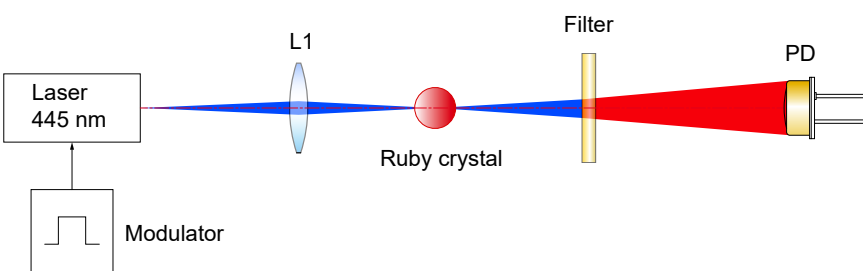
Ruby Crystal, $\text{Cr:Al}_2\text{O}_3$	Absorption Spectrum	Emission Spectrum
Lifetime of excited state	Einstein Coefficient for Spontaneous Emission	Blue Laser
Spectrometer	Spontaneous Emission	Optical Pumping



The invention of the Ruby Laser by Theodore Maiman in 1960 initiated the era of photonics technologies. This exciting experiment steps into the footmarks and tracks of famous scientists and provides a comprehensive inside of fundamental quantum optics. Although the Ruby Laser did not find great application it is still the first Laser system which is introduced to students as first invented Laser. By means of a couple of simple components great physics can be demonstrated. Due to the broad absorption bands of the Ruby crystal peaking around 405 nm as well as 560 nm either blue or green emitting LED or laser diodes can be used as excitation source. However, here a blue laser diode is used which emits less than 5 mW at a wavelength of 445 nm.



When Theodore Maiman laid out his first project proposal for funding, he received quite a lot of criticism. Although no laser has been brought to operation to that time, it was known based on the calculation of Schalow and Townes that the laser process requires a population inversion. That means that the number of excited Ruby atoms with energy E_2 must be greater than that of E_1 . Because the laser end level is the same as the start level a population inversion should not be possible. However, it turned out, that the level E_2 is a so called metastable state and the probability of optical transition from here down to the ground state are is quite low. That means further that the lifetime of the level E_2 is that high, that for a short moment a population inversion can be maintained. The starting lasing process significantly depletes the population of level E_2 by stimulated emission and consequently ceases the population inversion. That is the reason why the Ruby laser operates in pulsed mode only. Nevertheless, it was a great success for Theodore Maiman to discover the first laser.



ode laser on and off. A reference signal of the modulator is connected to the second channel of an oscilloscope. The signal of the photodiode is connected to the first channel of the oscilloscope. The trigger is set to the modulation signal channel. The decay time of the fluorescence signal is in the range of milliseconds so that a simple oscilloscope can be used to measure the lifetime of the excited state. Instead of the photodiode the fibre of the provided spectrometer is used, allowing the recording of the fluorescence spectrum.

Fig. 4.65: Principle setup

The light of the blue emitting diode laser is focused by the Lens L1 into the synthetic Ruby

crystal ball. The filter blocks the not absorbed pump radiation. The modulator switches the di-

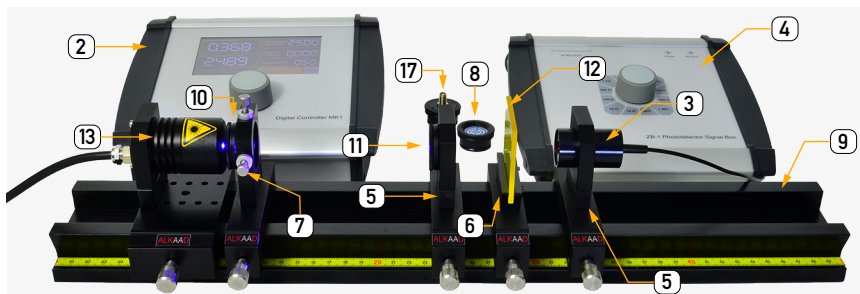
Keywords

Introduction

How it works

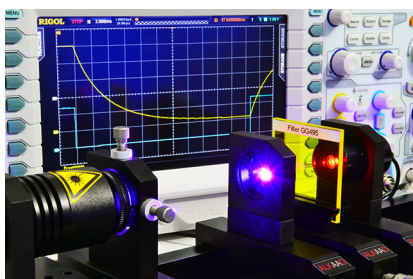
Optics Experiments

Description of the components



The Ruby crystal is mounted into a C25 mount (11) which is inserted into the mounting plate (5). The emission of the laser diode (13) is collimated and focused (10) into the crystal. The generated fluorescence passes the filter (12) which absorbs residual blue pump radiation and hits the photodiode. The created photo current is converted into a voltage by the junction box (4). For the initial alignment the target cross (8) is placed into one of the mounting plate and serves as reference for the optical axis.

Lifetime of Excited State



The blue diode laser is periodically switched on and off shown by the blue track of the oscillogram. The yellow track shows the fluorescence signal of the Ruby crystal. To determine the lifetime of the excited state the fluorescence signal after switching off the excitation is important. The time when the signal decreases to 1/e of its initial intensity is defined as lifetime Δt . The inverse value of it is the Einstein coefficient for spontaneous emission. The Fig. 4.67 shows such an example in which the value of the lifetime Δt has been measured to be 3.6 ms.

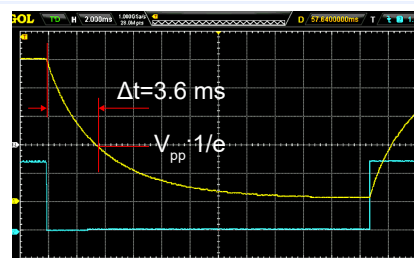


Fig. 4.67: Determine the lifetime of the excited state

Fluorescence Spectrum

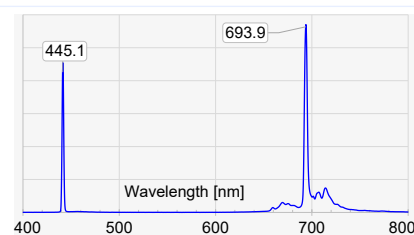
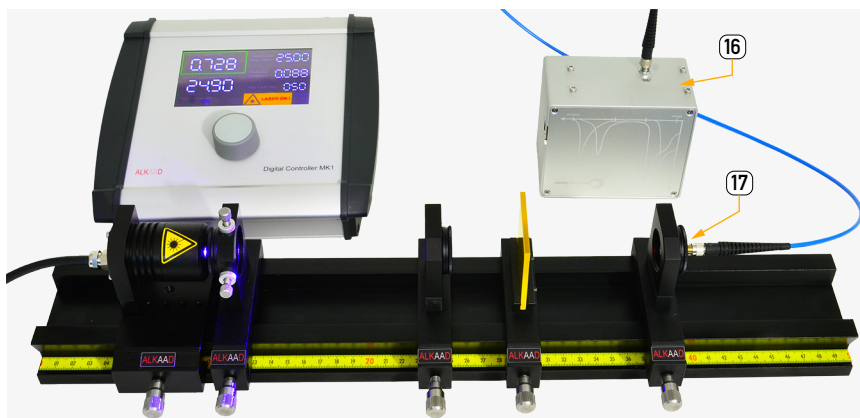


Fig. 4.68: Ruby fluorescence spectrum

The fibre of the optional spectrometer (15) is connected to the fibre holder (16) and the fluorescence of the Ruby crystal is detected by the spectrometer. Due to the high sensitivity of the spectrometer no focussing lens is required. The spectrum (Fig. 4.68) shows beside the pump laser line the famous 694 nm Ruby Laser line.

Absorption Spectrum

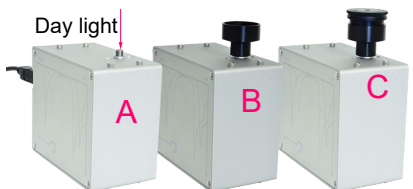


Fig. 4.69: The spectral absorption

The spectrometer allows to record the absorption spectrum of the Ruby crystal. By using the light of a simple light bulb a sequence the dark (A), reference (B, with adapter) and transmission (C with crystal) spectra are recorded and stored. The provided software calculates $T=(C-B)/(A-B)$ and $I-T$ yields the absorption spectrum (Fig. 4.70). Two main absorptions appear around 406 and 555 nm. At 694 nm a narrow dip appears, which is caused by the fluorescence already generated by the white probe light.

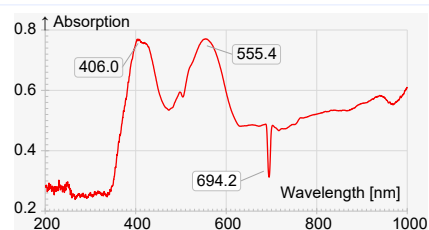


Fig. 4.70: Ruby absorption spectrum

PE-1500 Ruby Excited Lifetime & Spectroscopy consisting of:

Item	Code	Qty.	Description	Details page
1	CA-0450	1	BNC connection cable 1 m	130 (28)
2	DC-0040	1	Diode laser controller MK1	121 (4)
3	DC-0120	1	Si-PIN Photodetector, BPX61 with connection leads	123 (15)
4	DC-0380	1	Photodetector Junction Box ZB1	125 (31)
5	MM-0020	2	Mounting plate C25 on carrier MG20	93 (1)
6	MM-0060	1	Filter plate holder on MG20	94 (7)
7	MM-0090	1	XY adjuster on MG20	94 (8)
8	MM-0100	1	Target Cross in C25 Mount	94 (9)
9	MP-0150	1	Optical Bench MG-65, 500 mm	93 (8)
10	OC-0160	1	Collimator 445 nm in C25 mount	99 (12)
11	OC-0530	1	Ruby crystal in C25 mount	102 (32)
12	OC-0970	1	Filter GG495, 50 x 50 x 3 mm	104 (55)
13	OM-L445	1	Diode laser module 445 nm, 1 W	118 (55)
14	UM-PE15	1	Manual Ruby Spectroscopy	
Option (order separately)				
15	CA-0200	1	Oscilloscope 100 MHz digital, two channel	129 (19)
16	CA-0270	1	Fibre coupled spectrometer 200 - 1200 nm, USB	130 (26)
17	OC-0430	1	Fibre jacket in C25 mount	100 (21)

Highlights

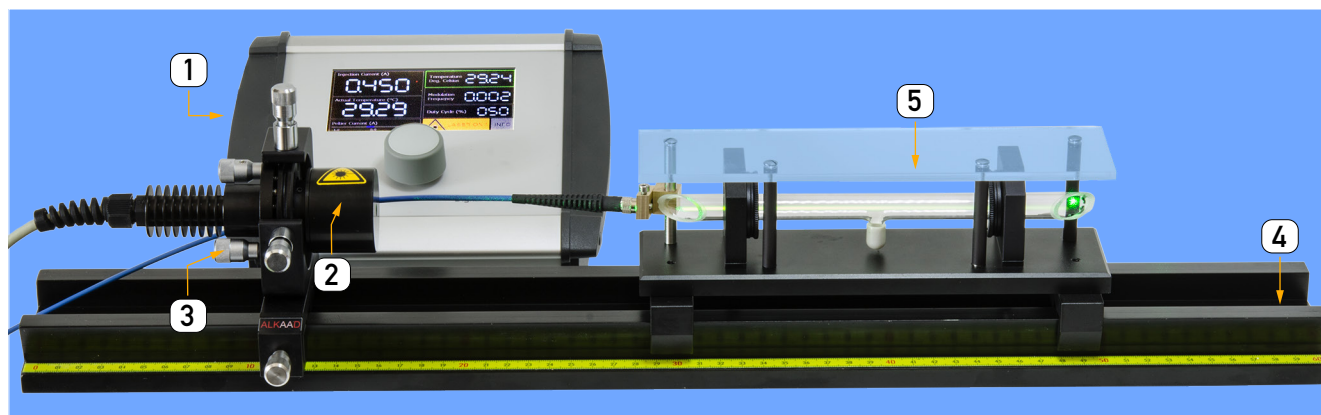
Basic experiment ★★

Simple but very meaningful and historical valuable

Intended institutions and users:

Physics Laboratory
Engineering department
Electronic department
Biophotonics department
Physics education in Medicine

PE-1600 Iodine Molecular Spectroscopy



Iodine Diatomic Molecule
Optical Pumping
Molecular Ground State

Molecule Energy Level
Fluorescence Spectrum
Uncertainty Principle

Stokes and Anti Stokes Emission
Dunham Coefficients
Franck Condon Principle

Keywords

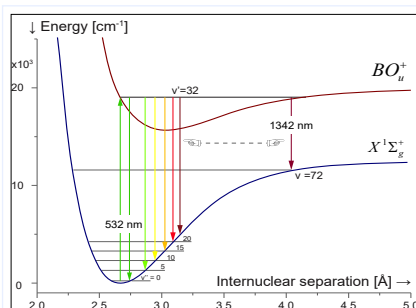


Fig. 4.71: Relevant Iodine molecule energy level

Molecular spectroscopy is one of the most important technologies to identify molecules in science, chemistry, biology and even in security applications. Precision spectroscopy, optical communication, modern length and frequency measurements using references and secondary frequency standards respectively based on stabilised laser. At present 12 optical frequencies in the visible and near infrared range are proposed by the “Comité International des Poids et Mesures (CIPM)”. Six of them use transitions

of Iodine molecules. For the time being the hyper fine transition of the iodine molecule a_{10} of the R(56)(32-0) is declared as reference with a relative uncertainty of $7 \cdot 10^{-11}$. In the Fig. 4.71 the transition (32-0) is shown. Hereby, is 32 the vibration quantum number of the excited BO_u^+ state and 0 those of the $X^1\Sigma_g^+$ ground state. However, a great variety of transitions to the ground state exist which will be one topic of interest within this experiment.

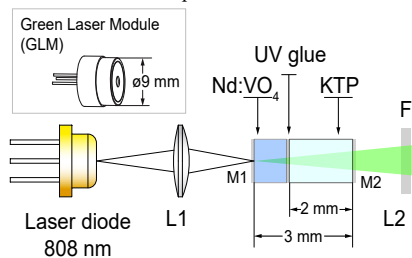


Fig. 4.72: Laser pointer, 532 nm radiation

Iodine is ideally suited since it consists out two identical atoms also termed as a diatomic molecule or also as dimer. Remarkably, opti-

cal transitions are only allowed between the electronic states of the molecule resulting in a clearer spectrum. Even more, with a suitable narrowband laser only one level is excited from which a series of transitions down into various vibrational levels of the ground state take place. In the past, expensive lasers have been used to study the properties of molecular Iodine. The inexpensive “green laser pointer” provides a wavelength at 532 nm which is ideal to excite the iodine molecule (Fig. 4.72).



However, the underlying generation of the green radiation is based on the frequency doubling of a diode pumped Nd:VO₄ laser. Such a laser has a gain bandwidth of 1 nm. Due to thermal drift of the cavity, the frequency doubled radiation also drifts in a range of 0.5 nm (530 GHz). However, the absorption width of the Iodine molecule due to the Doppler broadening of 437 MHz at 25°C is much smaller compared to the thermal drift of the excitation laser. Therefore the cavity of the “green laser” must be actively thermally stabilised.

The Iodine Cell

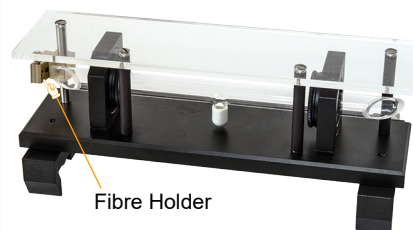


Fig. 4.73: Iodine Cell (8)

The essential part of this experiment is the Iodine cell. It consists of a 200 mm long (including the Brewster windows) quartz cell. By means of a special glass soldering technique the Brewster windows are vacuum sealed to the quartz tube. After baking out the cell at high temperatures the natural Iodine is distilled under ultra high vacuum via the fill stem into the cell and subsequently sealed. Generally, the fill stem acts also as a reservoir where the Iodine condensates as long as its temperature is slight-

ly less than the rest of the cell.

The valuable Iodine cell is protected by a plexi-glas cover. The cell is fixed with soft O-rings into the mounting plates. Even at room temperature, the Iodine forms diatomic molecules. The vapour pressure is about 20 Pa (0.2 mBar) at a temperature of 20°C. With two carriers the cell assembly can be attached to the optical rail.

The Laser Source



Fig. 4.74: Temperature stabilized GLM

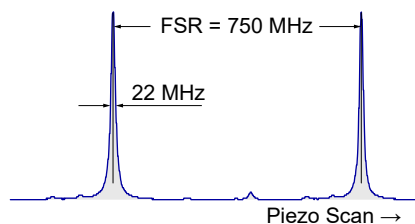


Fig. 4.75: Fabry Perot scan of the GLM

The green Laser Module (GLM) is mounted inside the housing between two Peltier elements. After connection with the DC-0044 Digital controller, the temperature can be set in a range from 10 to 40°C and kept constant within 0.01°C. The line width of the GLM is less than 22 MHz which can be proved by using the “LM-0300 Fabry Perot Spectral Analyser” on page 40. The maximum output power at 532 nm is 40 mW single mode and can be adjusted to a desired or recommended level.

Introduction

How it works

Optics Experiments

Digital Laser Controller



Fig. 4.78: GLM Controller DC-0010 HP

The laser is connected to the controller (CS) which maintains the temperature with an accuracy of 0.01°C and the injection current on 0.1 mA. A smooth temperature as well as current setting facilitates the tuning of the excitation laser to the respective transition. The GLM tunes with 0.004 nm or 4.5 GHz $^{\circ}\text{C}$. The Doppler broadened absorption line width is 0.437 GHz and thus the temperature setting must be less than tenth of a degree. To tune to the maximum of the absorption profile another factor of ten for

a stability of 0.01°C is suitable. The DC-0040 HP contains a MAX 1978 PID controller which is good for $\pm 0.001^{\circ}\text{C}$ accuracy. The DC-0040 HP has a USB bus and can be controlled by an external PC running the optional ES-0040 MK1 controller software.

All settings are done with the one knob selector and the touch screen. By tapping for instance the set temperature area, activates the knob to set the temperature in 0.01°C steps.

Fluorescence Measurement

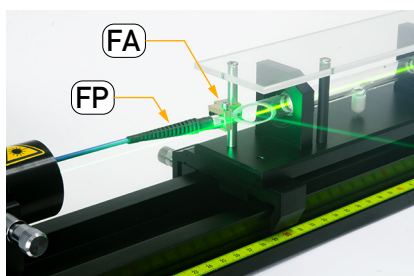


Fig. 4.76: Attached fibre of the spectrometer

The excitation or pump laser (2) is mounted into a 4 axes adjustment holder (3) to align the

beam centrally with respect to the iodine cell (5). The laser is connected to the controller (1) which maintains the temperature with an accuracy of 0.01°C and the injection current on 0.1 mA. A smooth temperature as well as current setting facilitates the tuning of the excitation laser to the respective transition. By means of an optical fibre probe (FP) the fluorescence light is guided to the optional spectrometer. The fibre probe is part of the optional spectrometer. If the customer already has such a spectrometer it can be used as well, however, the diameter of the ferrule should be 3.2 mm so that it fits into the fibre adapter (FA) which is attached to the support rod of the cell protective cover. The adapter is designed in such a way that the fibre looks into

the fluorescence path without being saturated by the pump light. After tuning the temperature to the strong visible fluorescence which appears as a greenish orange inside the cell. It takes a while to lock to the best temperature. In a first approach the set temperature is changed by lets say 2° . One observes the up and downs of the fluorescence as well as the actual temperature. The temperature is then set to this value and further adjusted. The power should remain unchanged (the more the better) while tweaking the temperature. The spectrometer should show already the first fluorescence spectrum and further refinements are done in 0.02°C steps for maximum amplitude.

Measurement example

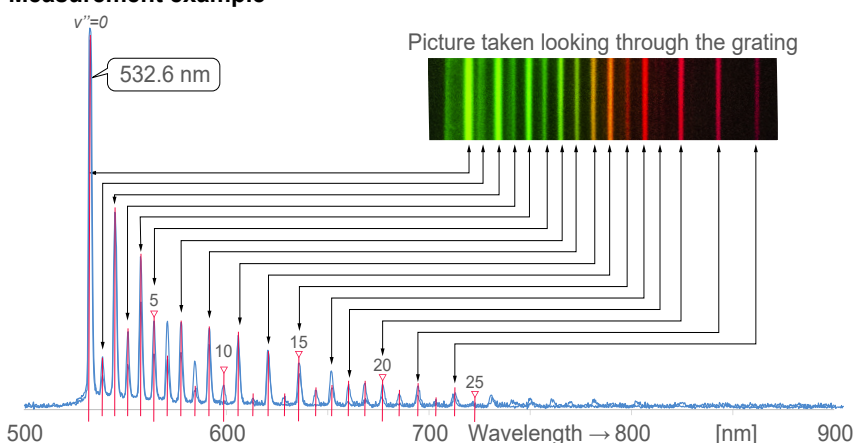


Fig. 4.77: Iodine Laser Induced Fluorescence (LIF)

To record the fluorescence spectrum an additional PC or tablet is required. The provided software allows the generation of a graphics or numerical data file which can be imported

to EXCEL for a more precise analysis and interpretation. The spectrum shown in Fig. 4.77 is an example of a measurement. The peak at the extreme left at 532.6 nm (the pump line)

represents a transition from $v'=32$ down to the vibrational ground state $v''=0$. From here onwards we can enumerate each peak by simple counting to the corresponding vibrational state. By using the given Dunham coefficients, the energy level can be calculated and drawn by the students (red lines). Finally the intensity of the fluorescence lines are related to the Franck Condon principle. For the transitions the Franck Condon factors are given and can be compared to the intensity distribution of the recorded LIF (Laser Induced Fluorescence) spectrum. The coloured line spectrum has been taken by using the provided grating with 600 lines/mm. The grating is placed directly in front of a digital camera, tilted a bit up or down to catch the variety of coloured lines of the first or second order. Just take a camera shot and download the image to your favourite image software and trim the image as shown in the beautiful and impressive Fig. 4.77. Compare the line structure of the spectrum with the coloured one and assign the transition with respect to the vibrational quantum numbers.

v''	Wavelength [nm]	v''	Wavelength [nm]	v''	Wavelength [nm]	v''	Wavelength [nm]	v''	Wavelength [nm]
0	532.6	7	577.6	14	628.5	21	686.0	28	751.2
1	538.7	8	584.5	15	636.3	22	694.9	29	761.1
2	544.9	9	591.5	16	644.2	23	703.8	30	771.3
3	551.2	10	598.7	17	652.3	24	713.0	31	781.6
4	557.7	11	605.9	18	660.5	25	722.3	32	792.1
5	564.2	12	613.3	19	668.9	26	731.7	33	802.8
6	570.8	13	620.8	20	677.4	27	741.4		

Table. 4.2: List of Transitions by vibrational quantum number v'' originating from $v'=32$ P(R)(32, v''), rotational level R not indicated.

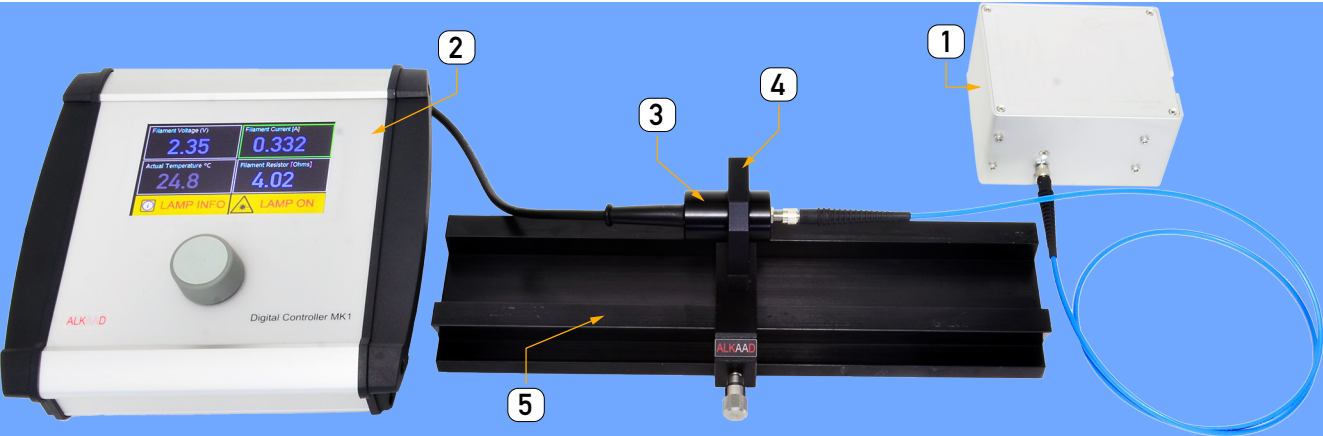
PE-1600 Iodine Molecular Spectroscopy consisting of:

Item	Code	Qty.	Description	Details page
1	DC-0010	1	Diode laser controller MK1-HP	121 (1)
2	LQ-0040	1	Green (532 nm) stabilized Laser, 40 mW	119 (3)
3	MM-0420	1	Four axes kinematic mount on carrier MG20	96 (25)
4	MP-0150	1	Optical Bench MG-65, 500 mm	93 (8)
5	OC-0460	1	Transmission grating 600 l/mm	100 (22)
6	OM-3010	1	Iodine cell on carrier	118 (53)
7	UM-PE16	1	Manual Iodine Spectroscopy	
Required Option (order separately)				
8	CA-0270	1	Fibre coupled spectrometer 200 - 1200 nm, USB	130 (26)

Highlights

Premium class experiment ★★★★★
Visible Laser Induced Iodine Fluorescence
Precise Spectroscopy
Intended institutions and users:
Basic / Medium / Advanced
Physics Laboratory
Engineering department
Electronic department


PE-1800 Planck's Law



Blackbody Radiation
Max Plank

Rayleigh-Jeans
Wien's approximation

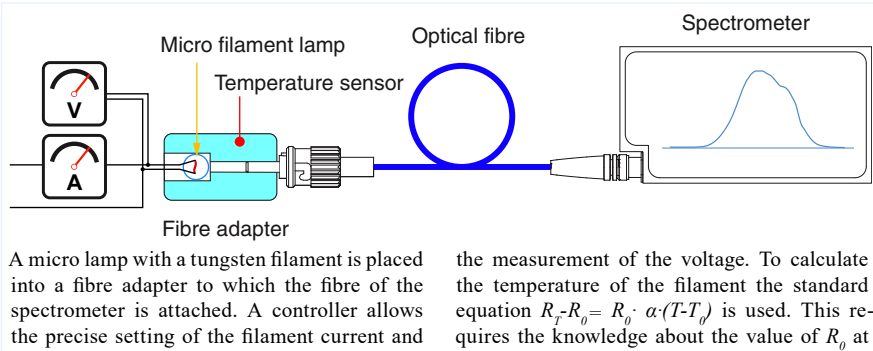
UV catastrophe
Temperature of the sun



It is a well known fact that hot bodies emitting optical radiation from ultraviolet to infrared. The spectrum shows a peak, which depends on the temperature of the body. This phenomenon attracted the scientist Rayleigh and Jeans to find an theoretical model for this. However, all their attempts failed and the correctly formulated solution predicted infinite power in the UV range of the spectral emission. It was Max Plank finding a way out

or the so called UV catastrophe by defining a new constant h and accidentally initiated a new physics, the quantum mechanics. In our experiment we will track some steps which lead at the beginning of the 20th century to a new understanding of the interaction with light and matter. We will use a kind of black-body radiator in form of an incandescent tungsten lamp. The emitted light is captured by a spectrum analyser in real time. With a precise current and voltage applied to the tungsten fila-

ment its temperature is determined. For a series of temperature values the emitted spectrum is recorded and stored for further analysis. The results are compared with Plank's law as well as the Wien's displacement law. Since the spectrometer is fibre coupled and very compact the spectrum of the sun can be recorded and based on the results of the previous measurements with the tungsten lamp the temperature of the sun is determined.



the temperature T_0 . For this purpose a temperature sensor measures the temperature T_0 of the switched off and cooled down lamp while the resistor R_0 is measured and displayed by the controller. After getting this data the spectrometer is connected to the lamp and a series of spectra is recorded. It should be mentioned that the spectrometer provides raw data without correction of the spectral sensitivity of it. For each recorded spectrum the temperature of the filament is known and the Plank's law can be calculated accordingly as reference.

Measurements

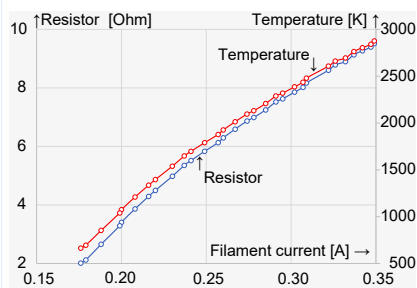


Fig. 4.79: Measurement of the filament resistor versus the filament current and determine its temperature

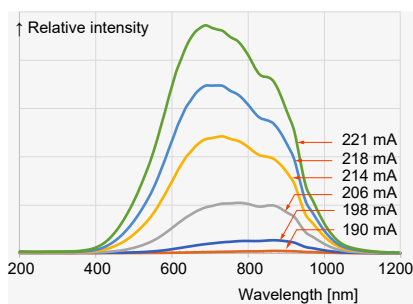


Fig. 4.80: Raw spectra at various filament currents

At the maximum permissible filament current of 0.35 A its temperature reaches 2886 °K. The Fig. 4.79 shows the measurement of the filament resistor for a series of currents. Since a micro lamp is used (3), the filament resistor is accordingly low and has a resistor of 0.75 Ohms at 300°K and reaches 9.7 Ohm at 2886 °K (0.350 A).

Highlights

Basic experiment ★★ ★
Simple but very meaningful

Intended institutions and users:
Physics Laboratory
Engineering department
Electronic department
Biophotonics department
Physics education in Medicine

PE-1800 Planck's Law consisting of:				
Item	Code	Qty.	Description	Details page
1	CA-0270	1	Fibre coupled spectrometer 200 - 1200 nm, USB	130 (26)
2	DC-0270	1	Filament and LED lamp controller	125 (26)
3	LQ-0440	1	Tungsten filament white light source	121 (17)
4	MM-0020	2	Mounting plate C25 on carrier MG20	93 (1)
5	MP-0130	1	Optical Bench MG-65, 300 mm	93 (7)
6	OC-0430	1	Fibre jacket in C25 mount	100 (21)
7	UM-PE18	1	Manual Planck's Law	